

STEROID AUTORADIOGRAPHIC ANALYSIS OF ANDROGEN-DEPENDENT  
TISSUE INTERACTIONS IN THE DEVELOPMENT OF  
MAMMALIAN PROSTATE GLANDS

A thesis  
submitted for the degree of Doctor of Science  
University of Tokyo

By

Hiroyuki Takeda

Zoological Institute, Faculty of Science,  
University of Tokyo

1986

## CONTENTS

	pages
Acknowledgements -----	1
General Introduction -----	2
Part I. Androgen-Binding Sites in the Rat Urogenital Sinus and Postnatal Prostate	
Introduction -----	5
Materials and Methods -----	7
Results	
Chapter 1. Androgen binding sites in fetal urogenital sinus -----	20
A. Androgen binding sites	
B. Competition experiments	
Chapter 2. Appearance of androgen binding sites and functional differentiation in postnatal prostatic epithelium -----	32
A. Androgen binding sites	
B. Acid phosphatase and non-specific esterase activities in the prostatic epithelium	
Discussion -----	43
Summary -----	47
Part II. Analysis of Prostatic Bud Induction by Brief Androgen Treatment in Fetal Rat Urogenital Sinus	
Introduction -----	48
Materials and Methods -----	49
Results -----	52

A. Induction of prostatic buds by continuous exposure to testosterone	
B. Prostatic bud formation after brief exposure to testosterone	
C. Incorporation of [ <sup>3</sup> H]testosterone in the mesenchyme	
Discussion -----	62
Summary -----	64
Part III. Behaviour of Androgen-Activated Mesenchymal Cells	
During Prostatic Bud Formation	
Introduction -----	65
Materials and Methods -----	67
Results	
Chapter 1. Visualization of X-chromosome mosaicism in testicular feminization mutant mice ----	71
Chapter 2. Behaviour of androgen-incorporating cells during prostatic morphogenesis -----	76
A. Prostatic bud formation in urogenital sinus of heterozygous female mice ( $X^{Tfm}/X^+$ )	
B. Autoradiographic analysis of the changes of mosaic pattern after androgen-treatment	
C. Effect of testosterone on the mesenchymal cell proliferation	
Discussion -----	94
Summary -----	99
General Conclusions -----	101
References -----	104

## CONTENTS OF FIGURES AND TABLES

	pages
PLATE 1 -----	10
Fig. 2 -----	11
PLATE 2 (Figs. 3-4) -----	17
PLATE 3 (Figs. 5-7) -----	23
Figs. 8a-e -----	25
PLATE 4 (Figs. 9-11) -----	27
PLATE 5 (Figs. 12a-d) -----	29
Table 1 -----	30
Table 2 -----	31
PLATE 6 (Figs. 13-16) -----	36
PLATE 7 (Figs. 17-22) -----	39
PLATE 8 (Figs. 23-28) -----	42
Fig. 29 -----	55
Fig. 30 -----	56
Fig. 31 -----	57
Fig. 32 -----	58
Fig. 33 -----	59
PLATE 9 (Figs. 34-36) -----	61
Fig. 37 -----	69
PLATE 10 (Figs. 38-40) -----	73
Table 3 -----	74
Table 4 -----	78
PLATE 11 (Figs. 41-43) -----	80
PLATE 12 (Figs. 44-45) -----	82

PLATE 13 (Figs. 46-48)	-----	87
Fig. 49	-----	88
Fig. 50	-----	89
PLATE 14 (Figs. 51-52)	-----	91
Table 5	-----	92

## ACKNOWLEDGEMENT

\*\*\*\*\*

I wish to express my deepest gratitude to Professor Takeo Mizuno of the University of Tokyo for his continuous guidance and encouragement during the course of this work. I am greatly indebted to Doctor Ilse Lasnitzki at Strangeways Research Laboratory in Cambridge for her helpful discussion and valuable advice. I also thanks Professor Masuo Suzuki of the University of Tokyo for his kind teaching on the analysis of mosaic pattern, Professor Walter E. Stumpf of the University of North Carolina for his technical suggestions, Doctor Shigeo Takeuchi, Doctor Sadao Yasugi and Mr. Hiroshi Fukamachi of the University of Tokyo for their kind advice.

## GENERAL INTRODUCTION

\*\*\*\*\*

There have been many works concerning the roles of sex steroids in embryonic development, morphogenesis, and expression of functional activity of mammalian sex organs. In male fetuses, androgens secreted by fetal testis alter the development of mesonephric tubules, Wolffian ducts, urogenital sinus, external genitalia and mammary glands, so that they undergo masculine morphogenesis (Jost 1965; Wilson, Griffin, George, and Leshin, 1981). Estrogens, at least initially, are not required for the development of female sex organs but are involved in the postnatal growth, morphogenesis and functional differentiation of female sex organs (Jost, 1965; Takasugi, 1976). Thus, the rudiments of sex organs drastically alter their developmental fates under the influence of sex hormones. Like other organs, these rudiments are composed of epithelial and mesenchymal components. In adulthood the epithelia of sex organs exhibit the organ-specific morphology and function. Since it has been well established that epithelial development is influenced by the inductive interactions with the surrounding mesenchyme in embryonic organs (for review, see Saxén et al, 1976 and Wessells, 1977), it has been

speculated that sex hormones exert their effects through epithelial-mesenchymal interactions.

Prostate glands, one of the male accessory sex organs, develop from the urogenital sinuses as epithelial buds projecting from the sinus epithelium into the surrounding mesenchyme. Earlier work (Lasnitzki and Mizuno, 1977) has shown that androgens induce prostate glands de novo both in male and female rat urogenital sinuses grown in organ culture, but that the response of the female sinuses declines with advancing fetal age. Experiments with epithelial-mesenchymal recombinates of androgen-treated and -untreated sinus tissues have suggested that the mesenchyme plays a decisive role in the formation of the fetal prostate gland and that the mesenchyme may be a target for androgens (Lasnitzki and Mizuno, 1979).

This concept is supported by the finding that in recombinates of urogenital mesenchyme and epithelium from normal and androgen-insensitive (Tfm) mice the stimulation of the epithelium depends on the presence of a normal, androgen-sensitive mesenchyme and that the genotype of the epithelium is irrelevant (Cunha and Lung, 1978; Lasnitzki and Mizuno, 1980a)

To make further clear the mechanism of the prostatic bud induction, I examined androgen binding sites in urogenital sinuses and the behaviour of mesenchymal cells after androgen-incorporation. In PART I, I demonstrated autoradiographically androgen binding sites in the rat



urogenital sinuses during prostatic bud formation (Chapter 1). Furthermore, I examined the role of the epithelial androgen receptor in the functional differentiation of the epithelium by enzyme histochemistry and recombination experiment with Tfm epithelium and wild-type mesenchyme (Chapter 2). In PART II, I precisely investigated the relationship between androgen-incorporation into the mesenchyme and prostatic bud induction by brief androgen-treatments. Finally in PART III, by recombination of autoradiographic techniques and the use of  $X^{Tfm}/X^+$  heterozygous female mice, I visualized X-chromosome inactivation mosaicism concerning the expression of androgen-receptors in the sinus mesenchyme of hetrozygous female mice and tried to reveal the behaviour of androgen-activated mesenchymal cells by examining the changes in mosaic pattern after androgen-treatments.

PART I.

ANDROGEN-BINDING SITES IN THE RAT  
UROGENITAL SINUS AND POSTNATAL PROSTATE

\*\*\*\*\*

Introduction

The epithelial-mesenchymal recombination experiments between androgen-treated and -untreated sinuses (Lasnitzki and Mizuno, 1979) or Tfm and wild-type sinuses (Cunha and Lung, 1978; Lasnitzki and Mizuno, 1980a) have supported that the mesenchyme is <sup>an</sup> actual target for androgens in androgen-induced prostatic morphogenesis. Since it is generally accepted that androgens exert their effects on target organs by way of specific receptor molecules, it is reasonable to postulate that the mesenchymal cells are the primary sites of androgen-receptor activity. In this context, it is quite important to reveal the distribution of androgen receptors in the urogenital sinus.

Autoradiography for diffusible substances such as steroid hormone has been supposed to be susceptible to various artifacts in that they are not covalently bound to macromolecules and loss or redistribution easily occurs during autoradiographic processings. These difficulties,

however, have been overcome by the introduction of the dry-mount and thaw-mount techniques with unfixed frozen sections (Stumpf, 1968; Stumpf and Sar, 1975) and it has been established that the nuclear uptake of steroid hormones shown by autoradiography is indicative of presence of a receptor system for the hormones (Sheridan, Buchanan and Anselmo, 1981).

In the PART I of the thesis, I revealed by steroid autoradiographic techniques the distribution of androgen-binding sites in the rat urogenital sinus and postnatal prostate. Moreover, to investigate the relationship between cytodifferentiation and androgen incorporation in the prostatic epithelium, I examined by enzyme histochemistry the appearance of acid phosphatase and non-specific esterase activities in the rat prostatic epithelium during normal development and in the recombinates of Tfm epithelium and wild-type mesenchyme.

## Materials and Methods

### Autoradiographic analysis

Wistar-Imamichi rats (Imamichi Institute for Animal Reproduction, Oomiya, Japan) were utilized in this study. The animals were mated during the night and copulation was confirmed by the presence of spermatozoa in the vaginal smears on the following morning. The conceptus was considered 0.5 days of gestation at 12 noon of this day. Gestation normally lasted 22 days and postnatal animals were considered 0 day on the day of birth. In male urogenital sinuses prostatic buds first appear between 18.5 and 19.5 days of gestation.

The following tissues were examined: urogenital sinuses and urinary bladders of 14.5-, 16.5-, 18.5- and 20.5-day male and female fetuses, and ventral prostatic lobes of 1-, 3-, 6-, 10-, 14-, 28- and 84-day-old male rat. In the rats over than 10 days, castration was carried out 2-3 days before sacrifice to reduce endogenous androgens.

#### 1. Labelling procedures

Tissues were isolated from the surrounding sheath of fat and connective tissues in Tyrode's solution supplemented with 10% fetal bovine serum and were explanted whole except for the postnatal tissues which were cut approximately 1 mm thick. They were incubated in a medium containing labelled

hormones according to a modified Trowell's technique (Trowell, 1959; Lasnitzki, 1965): the explants were placed on a Millipore filter with pore size of 1.2  $\mu\text{m}$ , which was arranged on a stainless-steel grid placed within a small culture dish. The fluid medium was added so as just to cover the Millipore filter. The culture dishes were then placed in Petri dishes humidified by wet paper filters. For incubation, the Petri dishes were stacked in a McIntosh jar (Baird & Tatlock Co., Chadwell Heath, Essex, England) and perfused with a mixture gas of 50%  $\text{O}_2$  and 5%  $\text{CO}_2$ . The incubation was performed at 37°C.

The culture medium used for labelling was Medium 199 with Earle's salts (Gibco Lab., Grand Island, NY, U.S.A.) supplemented with 5% fetal bovine serum and 2.5  $\mu\text{Ci/ml}$  [1,2,6,7- $^3\text{H}$ ]testosterone (94 Ci/mmol or 103 Ci/mmol, Amersham), or 2.5  $\mu\text{Ci/ml}$  [1,2,4,5,6,7- $^3\text{H}$ ]dihydrotestosterone (146 Ci/mmol, Amersham).

After 12 hours' incubation the explants were transferred to 30 ml Tyrode's solution and washed twice for 1.5 hours with shaking at room temperature to reduce non-specific binding of [ $^3\text{H}$ ]labelled hormones (Shannon, Cunha, Taguchi, Vanderslice and Gould, 1982). Following 3 hours' washing the explants were then placed into OCT compound (TISSUE-TEK II, Lab-Tek Division, Miles Lab. Inc., Naperville, IL., U.S.A.) or liver paste, quickly frozen in isopentan chilled with liquid nitrogen and were stored in liquid nitrogen.

## 2. Autoradiographic techniques

Dry-mount and thaw-mount autoradiographic techniques introduced by Stumpf and Sar (1975) were used.

### A. Dry-mount autoradiographic technique

Dry-mount autoradiographic technique consists of the following steps: (a) cryostat cut of thin sections, (b) freeze-drying of sections, (c) dry-mounting of freeze-dried sections on emulsion-precoated slides and (d) photographic processing and staining of the slides.

a. Cryostat cut of thin sections. The explants embedded in liver paste were cut in a cryostat (CRYO-CUT II, American Optical, Buffalo, NY, U.S.A.) at about  $-25^{\circ}\text{C}$ . Sections, 5  $\mu\text{m}$  thick, were transferred to a polyvial (Fig. 2E). The polyvials containing the frozen sections were put in the precooled sample chamber (Fig. 2A) kept within the cryostat.

b. Freeze-drying of sections. Figure 1 shows the whole view of the freeze-drying unit used in this study. The sample chamber and a cryosorption chamber (Fig. 2B) were assembled within a cryostat and transferred outside to a Dewar flask filled with dry ice-ethylene dichloride slush ( $-40^{\circ}\text{C}$ ) for the sample chamber and that filled with liquid nitrogen ( $-196^{\circ}\text{C}$ ) for the cryosorption chamber (Fig.1). A vacuum between  $10^{-4}$  and  $10^{-5}$  torr was achieved with oil diffusion pump (OD-3S, SHIMAZU Co., Kyoto, Japan) connected between the chamber and a rotary pump (GP-50, NAKAMURA SEISAKUSHO Co, Tokyo, Japan). An ionization gauge (IG-11,

# PLATE 1

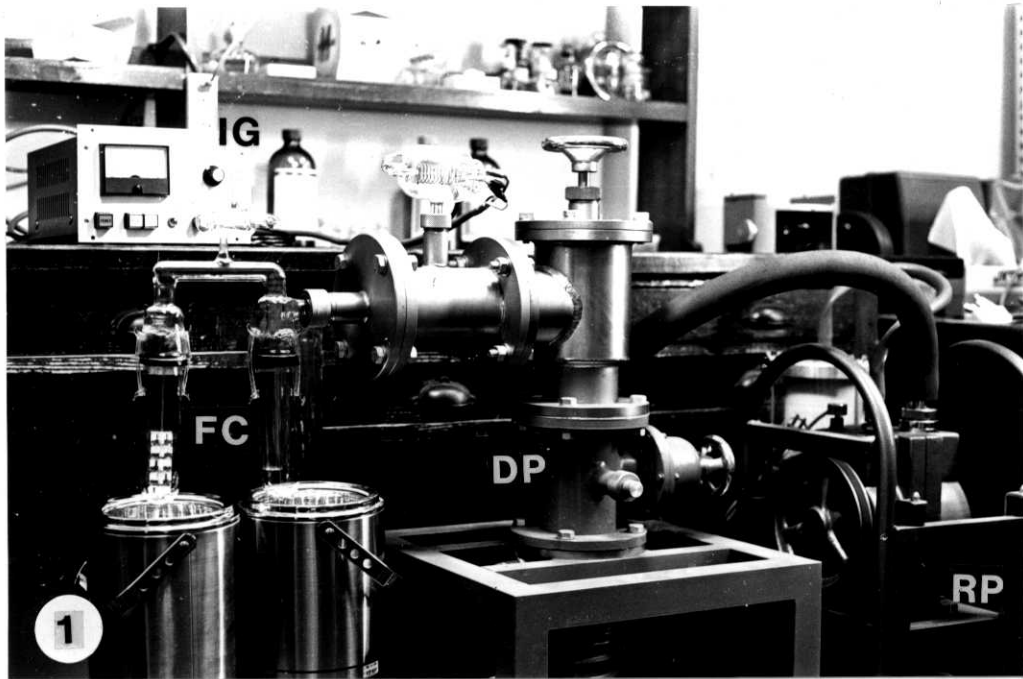


Fig. 1. Whole view of the freeze-drying unit used in the present study. A vacuum within the freeze-drying chamber (FC) was achieved with oil diffusion pump (DP) and rotary pump (RP). The vacuum was measured with an ionization gauge (IG).

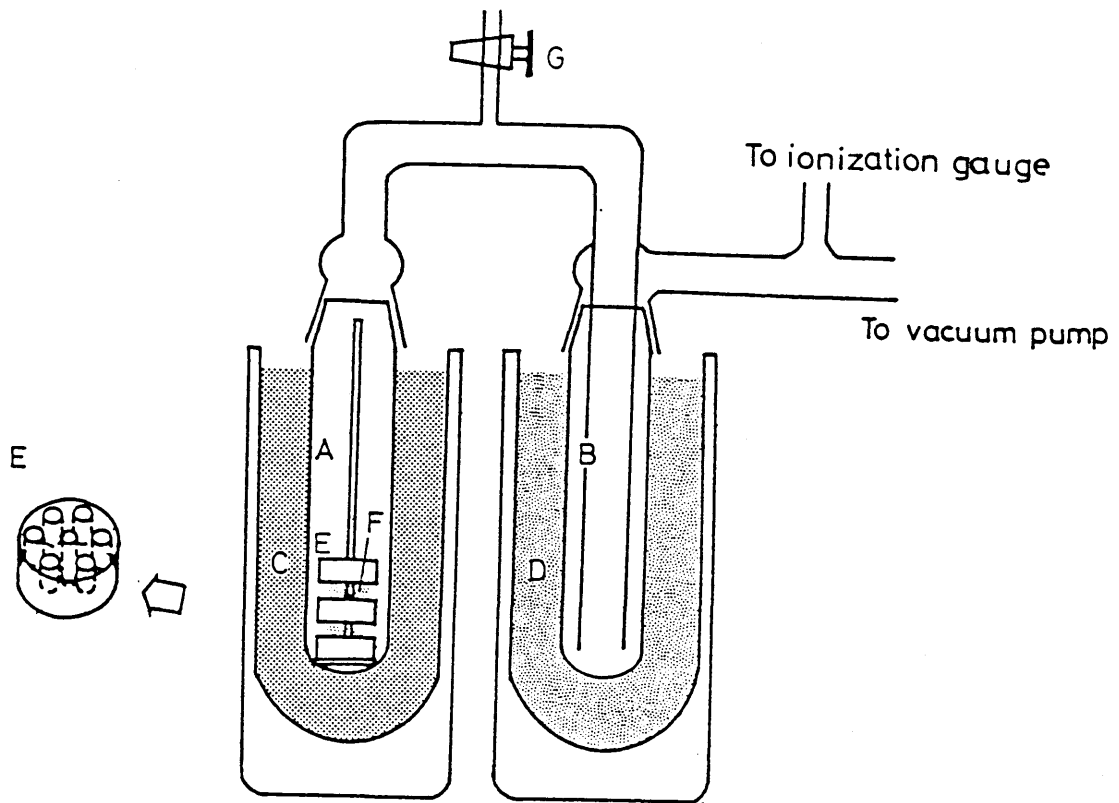


Fig. 2. Freeze-drying chamber. Sample chamber A, containing polyvials E stacked with mesh F, is immersed in dry ice-ethylene dichloride slush C. Cryosorption chamber B is immersed in liquid nitrogen D. The water evaporated from frozen sections is trapped in the cryosorption chamber. After freeze-drying, the vacuum is broken with dry nitrogen gas introduced through cock G.



SHIMAZU Co.) was used for the measurement of the vacuum within the chamber. Freeze-drying was terminated after 10 hours. One hour before breaking the vacuum with dry nitrogen gas, the sample chamber was removed from the coolant and allowed to equilibrate to room temperature, while the cryosorption chamber remained in liquid nitrogen. The polyvials containing the freeze-dried sections were removed and stored in a desiccator at room temperature.

c. Dry-mounting of freeze-dried sections. The freeze-dried sections were placed on a smooth and clean piece of Teflon with the thickness of 0.12 cm. Under safe light or complete darkness, an emulsion (NTB 3, Eastman Kodak Co., Rochester, NY., U.S.A.) -coated slide was placed over the Teflon piece with sections on it and both were pressed together. After release of the pressure, the sections adhered to the emulsion. The section-mounted slides were stored at 4°C for exposure in black slide boxes containing silica gel.

d. Photographic processing and staining of the slides. After 2 to 4 weeks' exposure the slides were removed from the slide boxes and the area of the sections was breathed on once or twice to improve adherence of the section to the emulsion. Before developing, the slides were fixed with 70% ethanol for 4 min. and were washed in deionized water. The slides were developed with Kodak D-19 developer in 1:1 dilution for 4 min. at 15°C, briefly rinsed in deionized water, fixed in Fuji Fix (Fuji Photofilm Co. Ltd., Tokyo,

Japan) for 10 min., rinsed in tap water for 10 to 15 min. and subsequently stained with methylgreen-pyronin or haematoxylin.

#### B. Thaw-mount autoradiographic technique

Frozen sectioning was performed as described above in the dry-mount autoradiographic technique. After frozen sectioning, sections were kept on the knife. Under safe light or complete darkness, an emulsion-coated slide was removed from a black slide box and placed over the sections on the knife. The frozen sections adhered to the emulsion just after melting due to the temperature of the slide. After mounting of the sections the slide was transferred to the slide box containing silica gel and was exposed at 4°C. Photographic processing and staining were done as described above in the dry-mount autoradiographic technique.

#### C. Comparison between the dry-mount and the thaw-mount autoradiography

In the thaw-mount autoradiographic procedures, wet interactions between tissues and emulsion may cause chemical artifacts and may cause varying degrees of diffusion of radioactive substances. Therefore, the thaw-mount autoradiography requires the dry-mount autoradiography as a control, in which the possibilities of chemical artifacts and diffusion are supposed to be minimized or eliminated.

Figures 3 show the dry-mount (a) and thaw-mount (b) autoradiogrammes of the urogenital sinuses of 18.5-day

female fetuses after incubation with [<sup>3</sup>H]testosterone. There was no significant difference between Figures 3a and 3b in the distribution and the number of silver grains. This result indicates that in these experimental conditions, the thaw-mount autoradiography can also demonstrate the localization of [<sup>3</sup>H]androgen as precisely as the dry-mount autoradiography. Moreover, the thaw-mount technique has the advantage that it saves time and the loss and damage of sections occurring after freeze-drying can be avoided. Therefore, the thaw-mount autoradiography was mainly applied to the following experiments and the dry-mount autoradiography was done as a control in a few selected explants.

#### D. Competition experiments

To assess the specificity of the binding of [<sup>3</sup>H]testosterone, I carried out competition experiments by applying a 200-fold excess of unlabelled hydrocortisone (Nakarai Chemical Ltd., Tokyo, Japan), 17 $\beta$ -oestradiol (Sigma Chemical Co., St Louis, MO, U.S.A.) and testosterone (Koch-Light Lab. Ltd., Bucks, England) in the culture medium containing 2.5  $\mu$ Ci/ml [<sup>3</sup>H]testosterone. After 12 hours' incubation the explants were processed according to the thaw-mount autoradiographic technique. The exposure period was 2 weeks. The urogenital sinuses of 16.5- and 18.5-day fetuses were analyzed.

For the quantitative analysis, at least 100 mesenchymal

cells, immediately adjacent to the ventral epithelium of the urogenital sinuses, were randomly selected and the number of silver grains per nucleus was counted. The results were statistically analyzed by student's t-test and differences  $P < 0.05$  were considered significant.

### Enzyme histochemistry

Tissues were fixed with ice-cold 2.5% glutaraldehyde in 0.1 M cacodylate buffer (pH 7.2-7.4) for 2 hours, washed overnight in several changes of 30% sucrose containing 1% gum arabic at 4°C and frozen in isopentan chilled with liquid nitrogen. Acid phosphatase was assessed at pH 5.2 by the azo-coupling method, with naphthol AS-BI phosphate (Sigma Chemical Co.) as the substrate and hexazotized p-rosaniline as the coupling dye and non-specific esterase was assessed at pH 6.8 by the azo-coupling method, with l-naphthyl acetate as the substrate and hexazotized p-rosaniline as the coupling dye (Lodja, Gossrau and Schiebler, 1979). Control studies were carried out on both two enzymes by omitting the substrate from the incubation medium and all controls were negative. The two enzymes were detected on frozen sections.

Explanation of PLATE 2

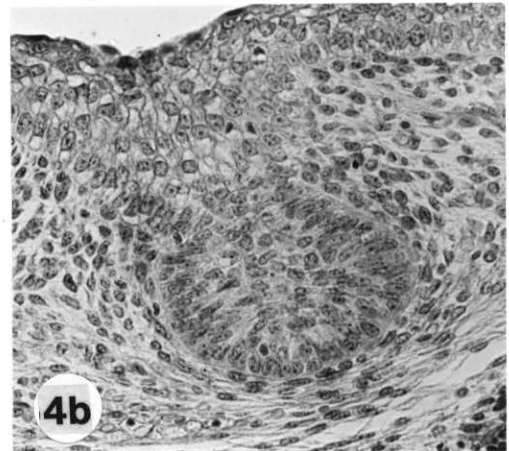
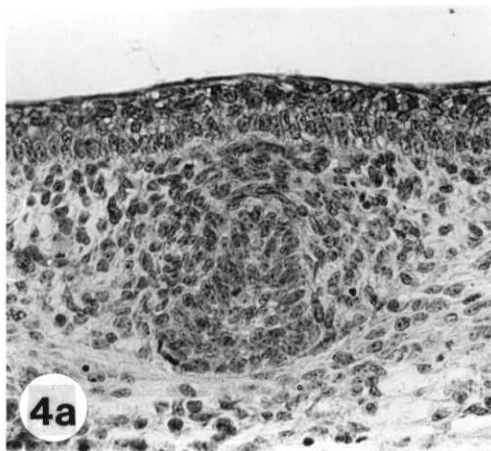
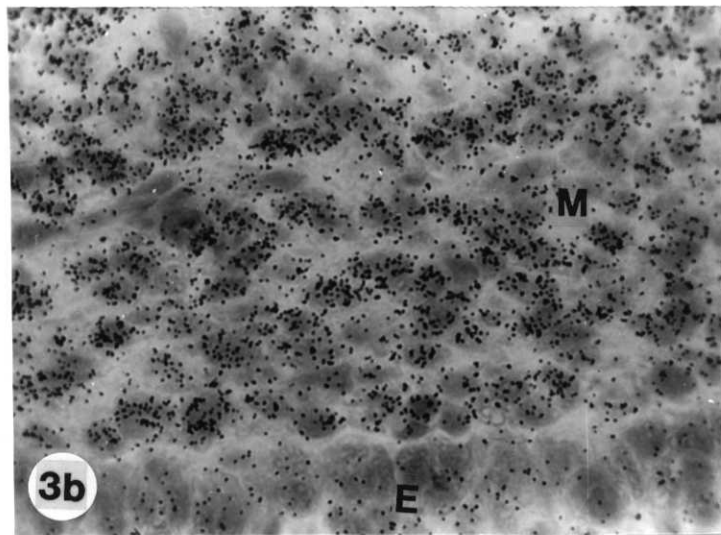
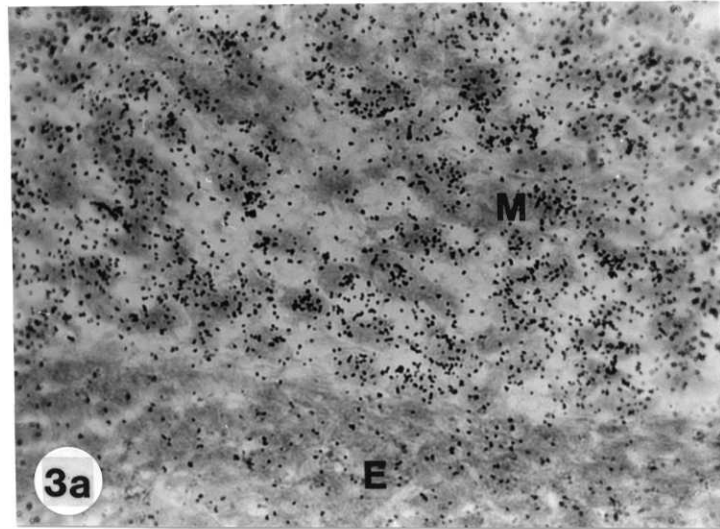
Abbreviations in figures

E, sinus epithelium; M, sinus mesenchyme

Fig. 3. Autoradiogrammes of urogenital sinuses of 18.5-day female fetuses incubated with [<sup>3</sup>H]testosterone. Frozen sections of the explant were processed according to the dry-mount (a) and thaw-mount (b) techniques. Exposure period: 3 weeks; X 550

Figs. 4. Section through pectoral skin of a 15.5-day male fetus. In normal wild-type mouse (X<sup>+</sup>/Y), mammary gland rudiment regressed (a), while it persisted in Tfm mutant mouse (b). X 280

# PLATE 2



Epithelial-mesenchymal recombination experiments  
using Tfm mutant mice

The mice carrying the Tfm mutation gene were kindly provided by Dr. Mary F. Lyon (MRC. Harwell, England). Mutant male ( $X^{Tfm}/Y$ ) fetuses were obtained by mating female carriers ( $X^{Tfm}/X^+$ ) with normal male ( $X^+/Y$ ). All male fetuses were handled individually. Urogenital sinuses from male 15.5-day-old mouse fetuses and from male 16.5-day-old rat fetuses were used.

1. Identification of Tfm mutant fetuses

Fragments of pectoral skin of all 15.5-day-old male fetuses used for the experiments were examined histologically for the presence of mammary gland rudiments. In wild-type male mice ( $X^+/Y$ ), mammary rudiments usually regress while they persist in mutant male mice ( $X^{Tfm}/Y$ ) (Figs. 4a and b).

2. Procedures of epithelial-mesenchymal recombination

Urogenital sinuses were treated with 0.06% collagenase for 30 minutes at 37°C, washed for 2 hours in three changes of Tyrode's solution supplemented with 50% fetal bovine serum, and separated into their epithelial and mesenchymal components.

The wild-type mouse epithelium or Tfm mouse epithelium

was associated with rat mesenchyme. They were cultured overnight in vitro to permit the re-establishment of firm adhesion, and then grafted beneath the kidney capsule of male athymic ICR nude mice (Charles River Japan Inc., Atsugi, Kanagawa, Japan). The grafts were harvested after 4 weeks' in vivo growth. For autoradiographic analysis, the hosts were castrated 3 days before sacrifice and the grafts were cut into small fragments and incubated with [<sup>3</sup>H]testosterone in vitro as described above.



## Results

There was no significant difference in the localization of [ $^3\text{H}$ ]testosterone or [ $^3\text{H}$ ]dihydrotestosterone through fetal stages. In this thesis the word "[ $^3\text{H}$ ]androgen" indicates both [ $^3\text{H}$ ]testosterone and [ $^3\text{H}$ ]dihydrotestosterone. Only [ $^3\text{H}$ ]testosterone was applied at postnatal stages.

### Chapter 1. Androgen binding sites in fetal urogenital sinus

#### A. Androgen binding sites

At 14.5 days of gestation neither male nor female sinuses incorporated [ $^3\text{H}$ ]androgens. However, when the period of exposure was prolonged to 3 months the mesenchyme showed weak nuclear labelling (Figs. 5a and b).

At 16.5 and 18.5 days of gestation the mesenchyme showed nuclear labelling while the epithelium remained unlabelled (Figs. 6a and b). There was no difference between male and female sinuses in the distribution of labelled cells. In the 18.5-day male sinuses the prostate glands started to develop as solid epithelial buds projecting from the sinus epithelium into the surrounding mesenchyme. At this stage, the intensity of labelling in the mesenchyme was similar in mesenchymal cells close to the developing prostatic buds and adjacent to the non-budding area of the epithelium (Fig. 7). In 20.5-day male sinuses the

mesenchyme showed, as before, distinct nuclear labelling which was particularly intense in the mesenchymal cells existing ahead of developing buds (Fig. 8d; Fig. 9). These mesenchymal cells may form the stroma of prostate glands in the course of development. The sinus epithelium and epithelium of the developing prostatic buds were still unlabelled (Fig. 8d; Fig. 9). In 20.5-day female sinuses the vagina is formed by separation from the dorsal epithelium. The dorsal mesenchyme surrounding the developing vagina incorporated [<sup>3</sup>H]testosterone to the same extent as that of the 18.5-day female sinus, while nuclear labelling of the ventral mesenchyme had diminished (Fig. 8e; Fig. 10). There was no uptake of [<sup>3</sup>H]androgens in epithelium or mesenchyme of the urinary bladder through fetal stages examined (Fig. 11).

#### B. Competition experiments

Figures 12a - d show the autoradiogrammes from the 18.5-day male incubated simultaneously with 2.5 µCi/ml [<sup>3</sup>H]testosterone and a 200-fold excess of unlabelled hormones. Quantitative data are presented in Tables 1 and 2. Similar competition patterns were obtained from 16.5- and 18.5-day fetal urogenital sinuses of both sexes: unlabelled testosterone abolished nuclear labelling completely, while cortisol had little effect on the distribution and the intensity of the nuclear uptake of [<sup>3</sup>H]testosterone.

Explanation of PLATE 3

Abbreviations in figures

E, sinus epithelium; M, sinus mesenchyme

Figs. 5. Autoradiogrammes of urogenital sinuses of 14.5-day male fetuses incubated with [<sup>3</sup>H]dihydrotestosterone (DHT).

(a) No nuclear concentration of [<sup>3</sup>H]DHT was observed.

Exposure period: 3 weeks; X 550 (b) Exposure period was increased to 3 months. The mesenchyme displayed weak nuclear labelling. X 550

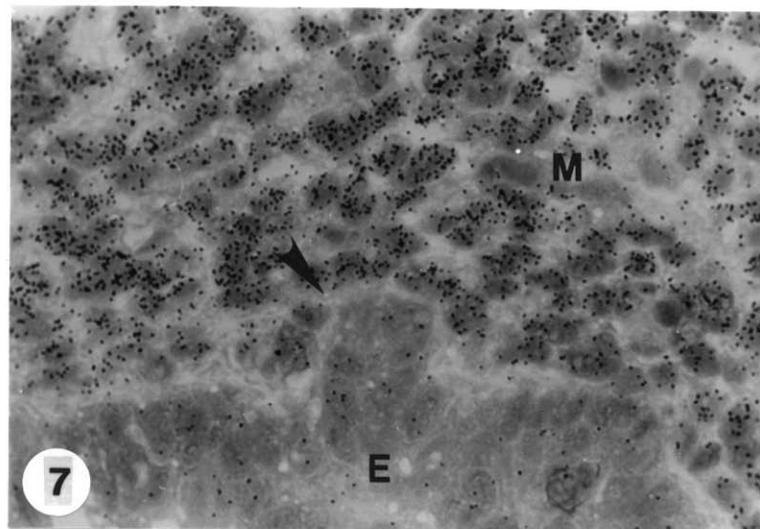
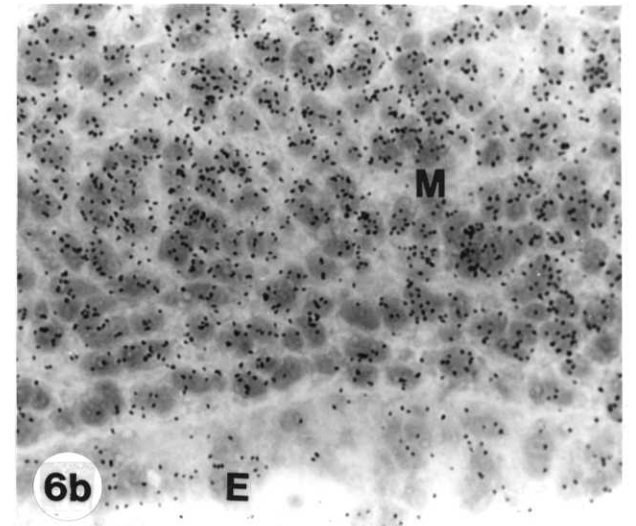
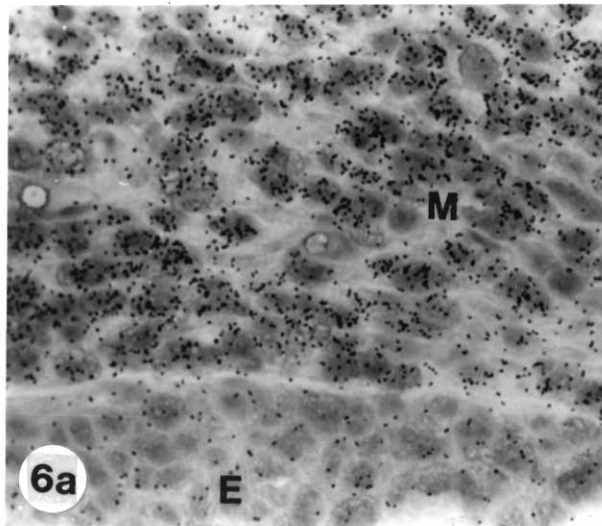
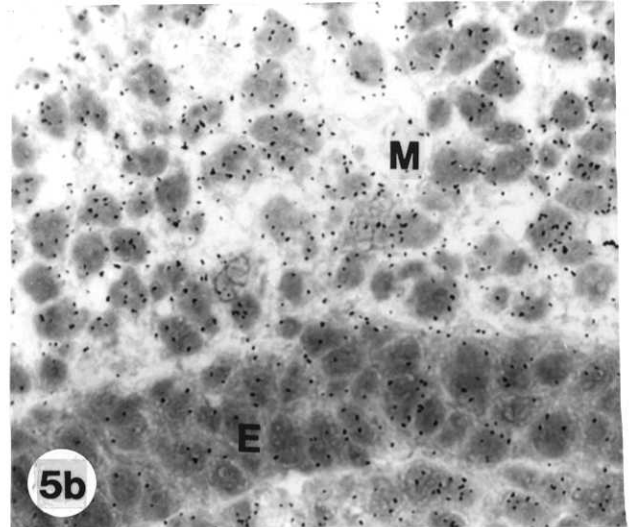
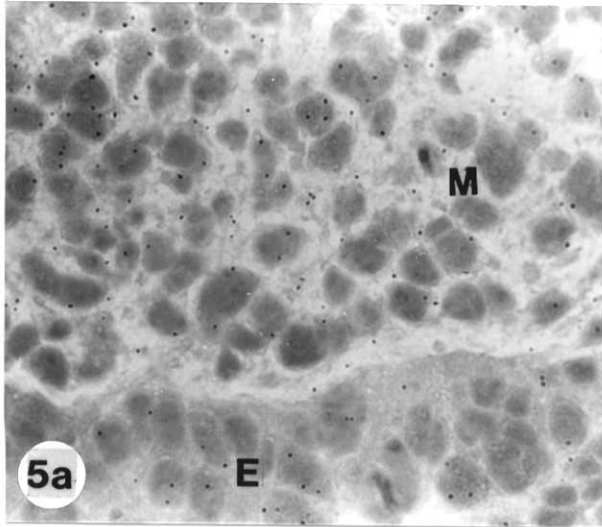
Figs. 6. Autoradiogrammes of urogenital sinuses of 16.5-day male (a) and female (b) sinuses incubated with

[<sup>3</sup>H]testosterone. Nuclear localization of [<sup>3</sup>H]testosterone was observed only in the mesenchyme in male and female fetuses. Exposure period: 2 weeks; X 550

Fig. 7. Autoradiogramme of urogenital sinus of an 18.5-day male fetus incubated with [<sup>3</sup>H]dihydrotestosterone. A prostatic bud (allow) developed from the sinus epithelium.

Note that the labelled cells are uniformly distributed throughout the mesenchyme irrespective of bud. Exposure period: 2 weeks; X 550

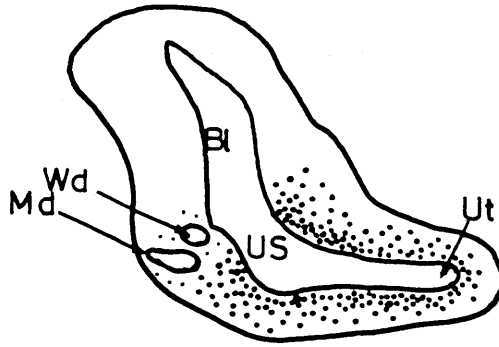
# PLATE 3



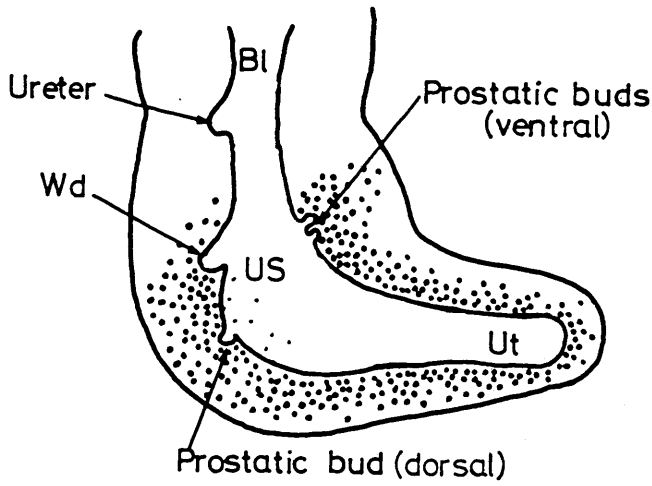
Figs. 8. Distribution of androgen-labelled cells in the urogenital sinuses of (a) male and female fetuses at 16.5 days of gestation (dg), (b) male fetuses at 18.5 dg, (c) female fetuses at 18.5 dg. (d) male fetuses at 20.5 dg and (e) female fetuses at 20.5 dg after incubation with [<sup>3</sup>H]testosterone. Schematic drawings were prepared from autoradiograms of longitudinal sections. The black dots represent the cells which concentrate [<sup>3</sup>H]testosterone in their nuclei. The relative intensity of labelling is indicated by the size of the dots, and the number of labelled cells by the number of dots. Bl, urinary bladder; Md, Mullerian duct; US, urogenital sinus; Ut, urethra; Wd, Wolffian duct; PB, prostatic buds.

# Figs. 8

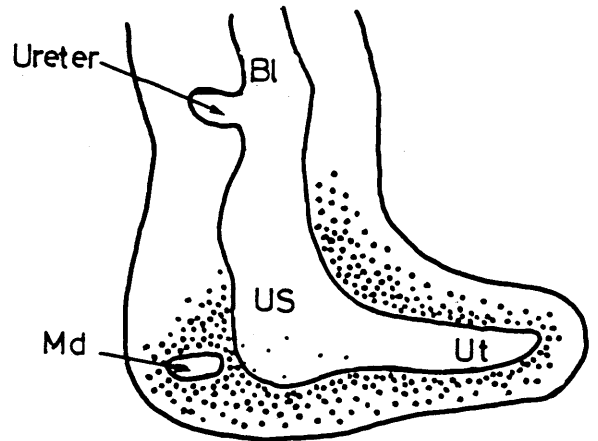
a. 16.5 d.g. male and female



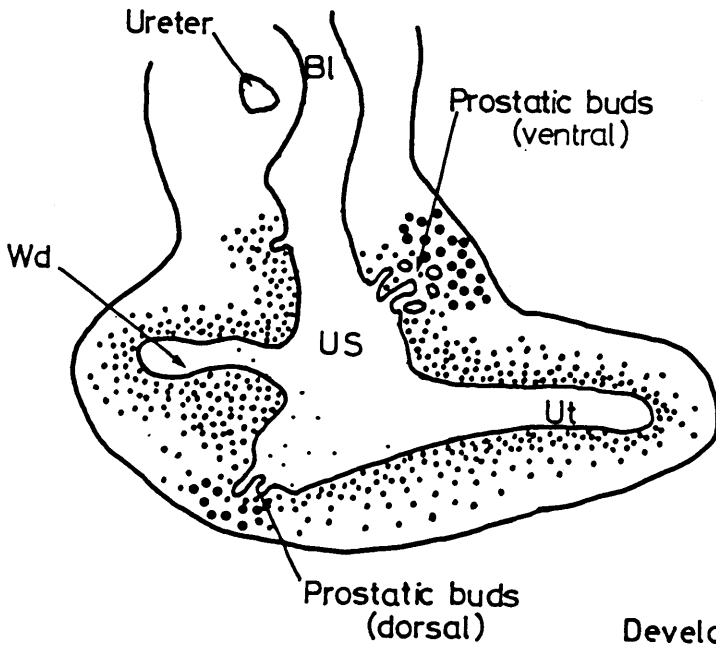
b. 18.5 d.g. male



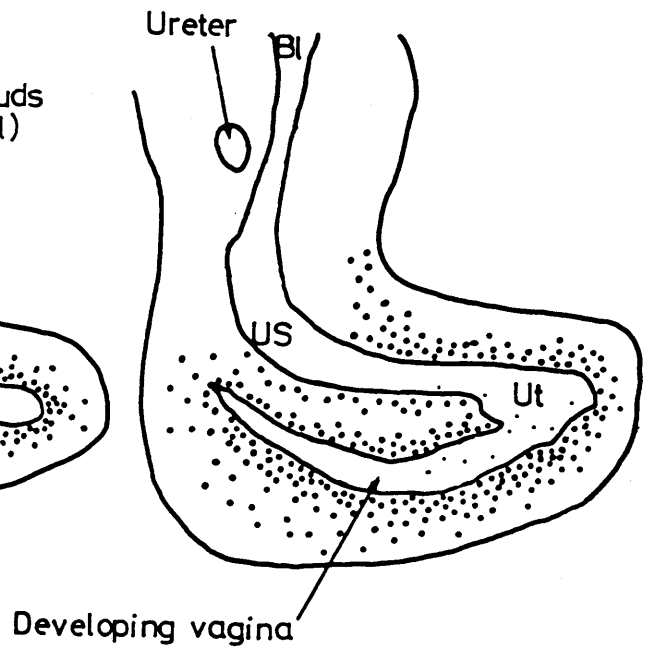
c. 18.5 d.g. female



d. 20.5 d.g. male



e. 20.5 d.g. female



Explanation of PLATE 4

Abbreviations in figures

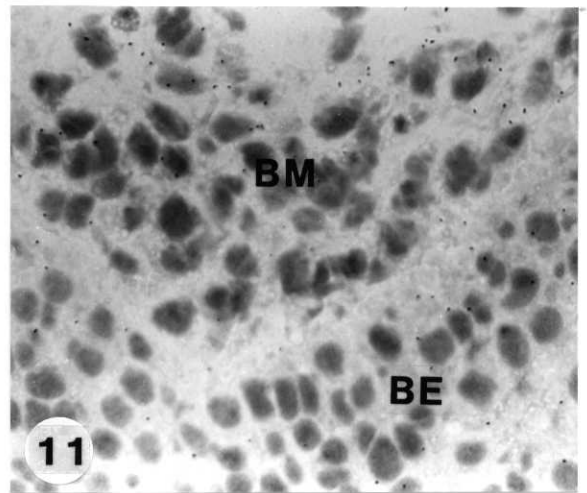
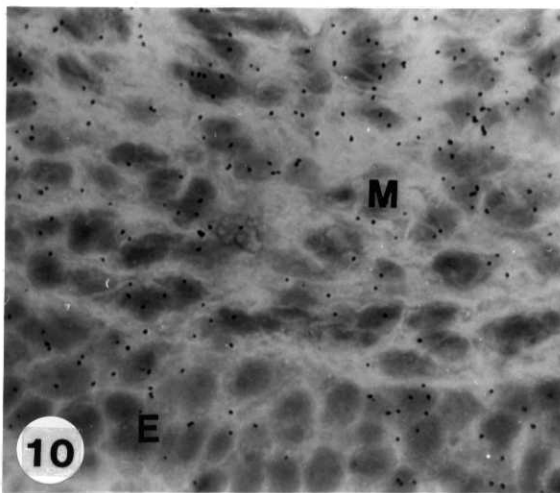
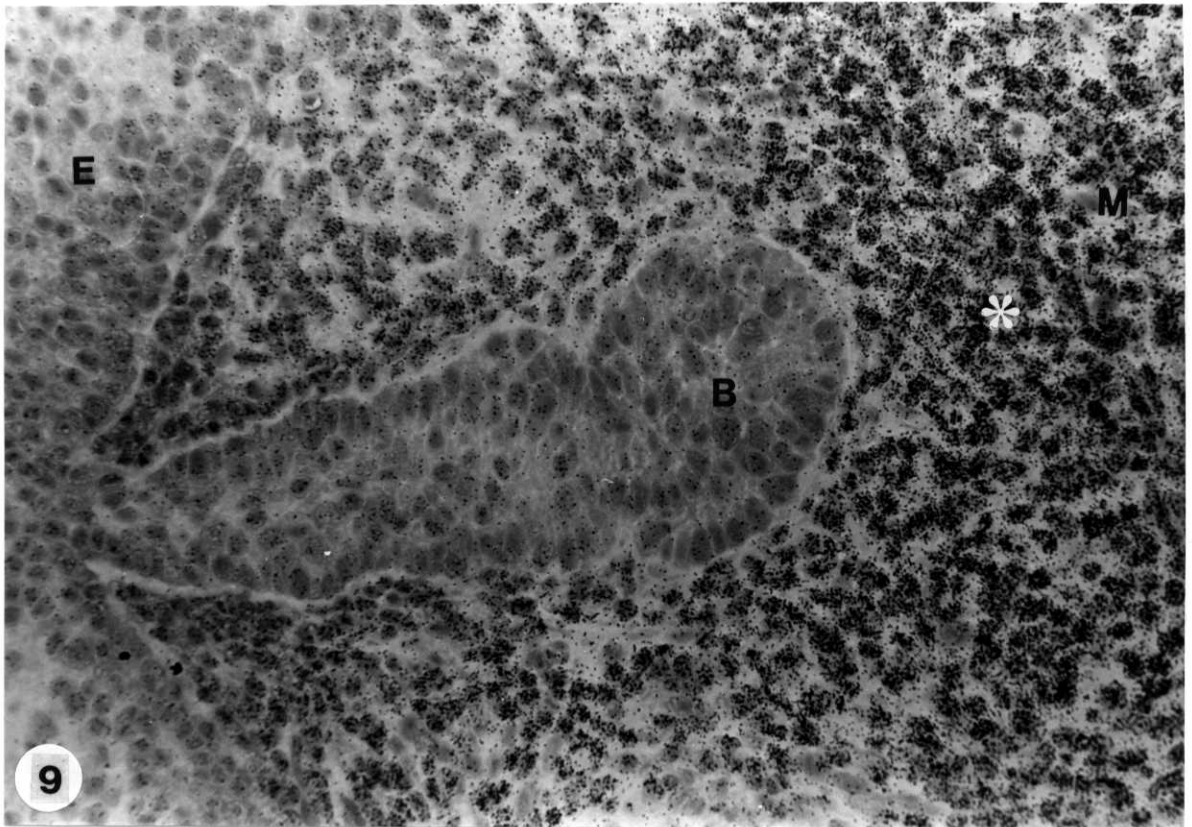
E, sinus epithelium; M, sinus mesenchyme; B, prostatic bud;  
BE, urinary bladder epithelium; UM, urinary bladder  
mesenchyme

Fig. 9. Autoradiogramme of urogenital sinus of a 20.5-day male fetus incubated with [<sup>3</sup>H]testosterone. Note that the mesenchymal cells ahead of the elongating prostatic bud are intensely labelled (\*). Exposure period: 3 weeks; X 400

Fig. 10. Autoradiogramme of urogenital sinus (ventral side) of a 20.5-day female fetus incubated with [<sup>3</sup>H]testosterone. The intensity of mesenchymal labelling was greatly decreased. Exposure period: 2 weeks; X 550

Fig. 11. Autoradiogramme of urinary bladder incubated with [<sup>3</sup>H]testosterone. Nuclei of bladder epithelium and mesenchyme did not uptake [<sup>3</sup>H]testosterone. Exposure period: 4 weeks; X 550

# PLATE 4





## Explanation of PLATE 5

Abbreviations in figures

E, sinus epithelium; M, sinus mesenchyme

Figs. 12. Autoradiogrammes of urogenital sinus of an 18.5-day male fetus incubated with 2.5  $\mu\text{Ci/ml}$  [ $^3\text{H}$ ]testosterone only (a) and incubated simultaneously with 2.5  $\mu\text{Ci/ml}$  [ $^3\text{H}$ ]testosterone and 200-fold excess of unlabelled hydrocortisone (b), unlabelled oestradiol (c) and unlabelled testosterone (d). Quantitative data are presented in Table 1 and 2. Exposure period: 2 weeks; X 550

# PLATE 5

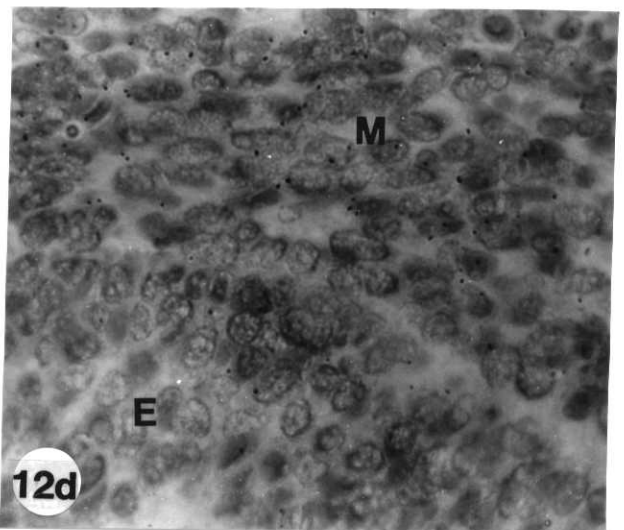
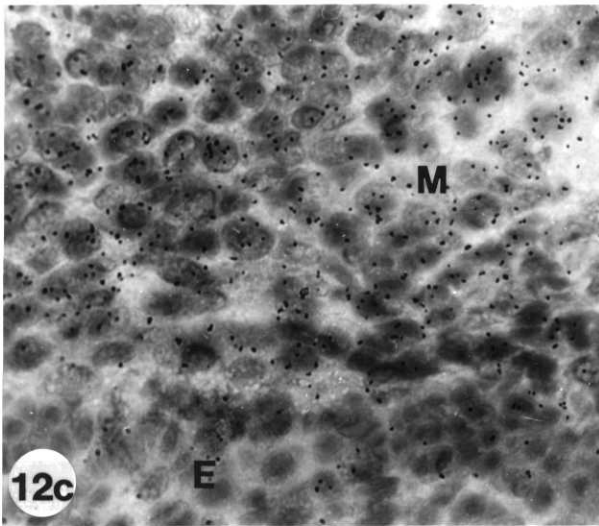
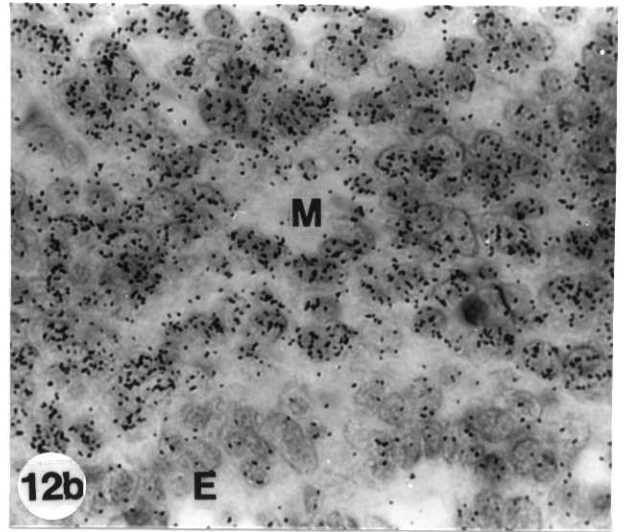
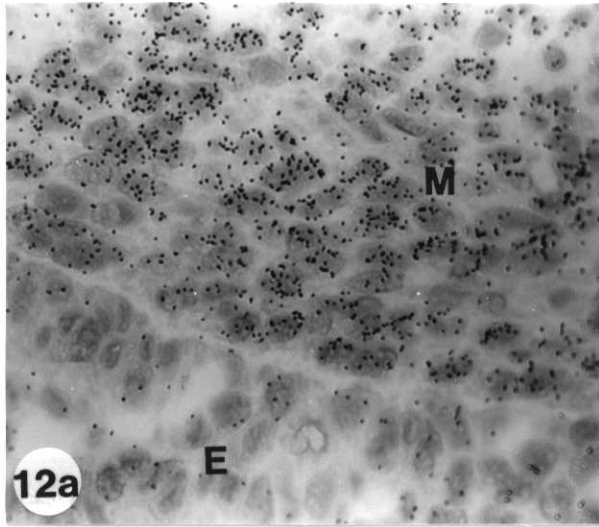


Table 1. Quantitative comparison of competition experiments in 16.5-day fetal urogenital sinuses.

Hormones added	Sex	No. of explants	Total No. of counted cells	Average grains per nucleus
$^3\text{H}$ -testosterone only	male	3	300	9.1 ± 3.4
	female	3	300	6.7 ± 3.2
$^3\text{H}$ -testosterone plus 200-fold of hydrocortisone	male	3	300	8.6 ± 3.2 <sup>a</sup>
	female	3	300	6.9 ± 2.8 <sup>a</sup>
$^3\text{H}$ -testosterone plus 200-fold of oestradiol	male	2	220	2.2 ± 1.8 <sup>b</sup>
	female	3	302	1.8 ± 1.8 <sup>b</sup>
$^3\text{H}$ -testosterone plus 200-fold of testosterone	male	2	200	0.5 ± 0.8 <sup>b</sup>
	female	3	310	0.4 ± 0.8 <sup>b</sup>

Values represent the mean ± S.D.

<sup>a</sup> No significant difference from the average observed for explants incubated with  $^3\text{H}$ -testosterone only. ( $P > 0.05$ ; t-test)

<sup>b</sup> Significantly different from the average observed for explants incubated with  $^3\text{H}$ -testosterone only. ( $P < 0.05$ ; t-test)

Table 2. Quantitative comparison of competition experiments in 18.5-day fetal urogenital sinuses.

Hormones added	Sex	No. of explants	Total No. of counted cells	Average grains per nucleus
$^3\text{H}$ -testosterone only	male	3	300	9.2 ± 3.6
	female	3	300	8.5 ± 3.3
$^3\text{H}$ -testosterone plus 200-fold of hydrocortisone	male	3	300	8.7 ± 3.2 <sup>a</sup>
	female	3	300	6.9 ± 3.1 <sup>b</sup>
$^3\text{H}$ -testosterone plus 200-fold of oestradiol	male	3	300	2.2 ± 1.7 <sup>b</sup>
	female	3	300	1.7 ± 1.8 <sup>b</sup>
$^3\text{H}$ -testosterone plus 200-fold of testosterone	male	2	200	0.4 ± 0.7 <sup>b</sup>
	female	3	300	0.5 ± 0.7 <sup>b</sup>

Values represent the mean ± S.D.

<sup>a</sup> No significant difference from the average observed for explants incubated with  $^3\text{H}$ -testosterone only. ( $P > 0.05$ ; t-test)

<sup>b</sup> Significantly different from the average observed for explants incubated with  $^3\text{H}$ -testosterone only. ( $P < 0.05$ ; t-test)

Oestradiol reduced the intensity of the nuclear labelling to 20-30%.

## Chapter 2. Appearance of androgen binding sites and functional differentiation in postnatal prostatic epithelium

### A. Androgen binding sites

In the ventral prostate of 1- to 6-day-old rats nuclear uptake of [<sup>3</sup>H]testosterone was observed in the mesenchyme. The epithelial buds which were still compact without canalization contained few labelled cells (Fig. 13). Uptake of [<sup>3</sup>H]testosterone by the prostatic bud epithelium was first seen at 10 days after birth when the epithelial buds began to canalize. The onset of [<sup>3</sup>H]testosterone binding in the epithelium appeared to precede the canalization of prostatic buds; the epithelial cells of some uncanalized buds exhibited androgen binding and the epithelial cells of canalized buds were consistently positive for androgen binding (Fig. 14). At this stage, the mesenchymal cells surrounding the buds were still labelled (Fig. 14).

By 4 weeks of age, the prostatic epithelium had differentiated into a columnar secretory epithelium typical for the adult prostate and exhibited intense nuclear labelling, while that of the surrounding mesenchyme was less intense (Fig. 15). This pattern of incorporation continued

into adulthood (Fig. 16).

B. Acid phosphatase and non-specific esterase activities in the prostatic epithelium

To know the timing of functional differentiation of the prostatic epithelium, I studied the appearance of acid phosphatase and non-specific esterase activities in the epithelium during normal development by means of enzyme histochemistry. The activities of the two enzymes in the epithelium first appeared at about 10 days after birth. The appearance of the activities seemed to correlate with the canalization of prostatic buds; that is, the epithelial cells of canalized buds were consistently positive for both two enzymes, while those of uncanalized buds were negative (Figs. 17-20). The two enzyme activities in the epithelium could be detected into adulthood, while the mesenchyme surrounding the epithelium exhibited no activity at any postnatal stage of development (Figs. 21 and 22).

To investigate whether the appearance of these enzyme activities would require androgens in the epithelium, I tried the histochemical analysis on the recombinates composed of the sinus epithelium of a 15.5-day-old Tfm mouse fetus and the sinus mesenchyme of a 16.5-day-old wild-type rat fetus. After 4 weeks' culture beneath the kidney capsule of a male host, prostate-like acini have developed, many of which showed acid phosphatase and non-specific

esterase activities as the wild-type epithelium (Figs. 23-26). The autoradiographic analysis confirmed that the Tfm epithelium, showing prostate-like structure, did not incorporate androgens while mesenchyme and the wild-type epithelium showed nuclear labelling (Figs. 27 and 28).

## Explanation of PLATE 6

### Abbreviations

E, prostatic epithelium; M, mesenchyme

B, prostatic bud; L, lumen

Fig. 13. Autoradiogramme of 6-day old rat ventral prostate incubated with [<sup>3</sup>H]testosterone. The uptake of [<sup>3</sup>H]testosterone by the mesenchyme was maintained, while the prostatic buds were not labelled. Exposure period: 3 weeks; X 820

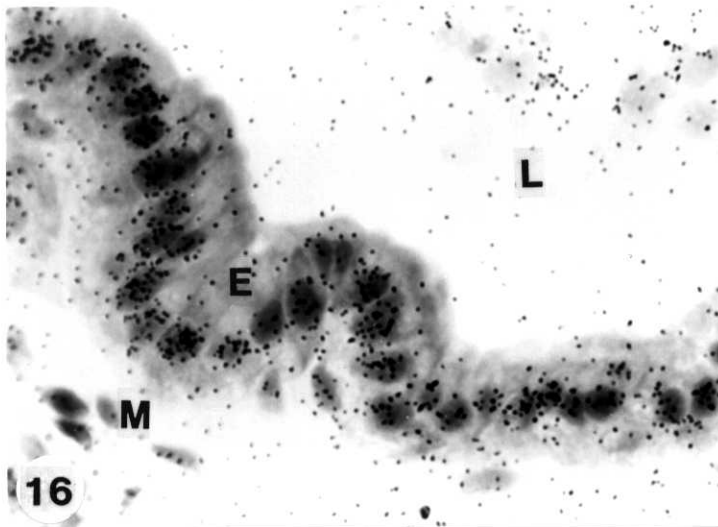
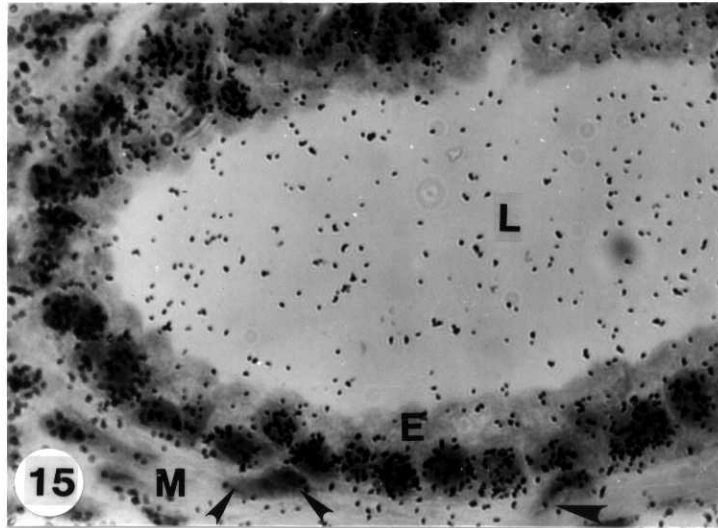
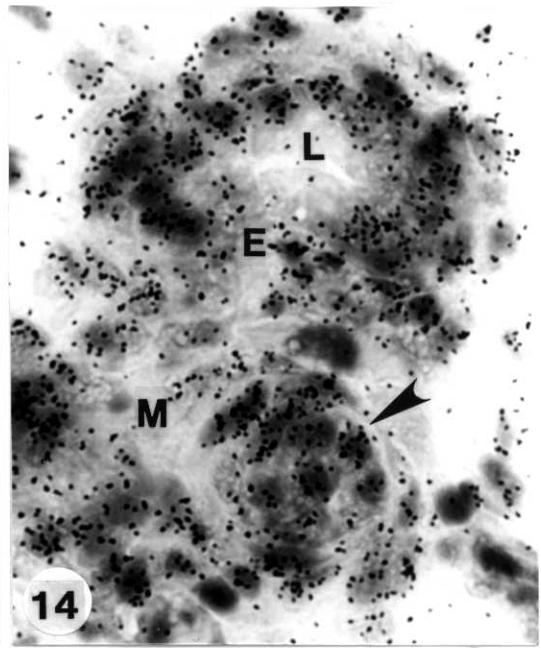
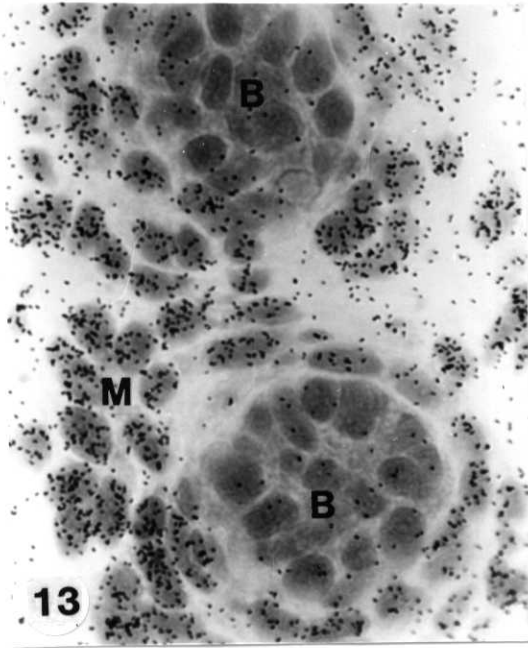
Fig. 14. Autoradiogramme of 10-day old rat ventral prostate incubated with [<sup>3</sup>H]testosterone. Lumen developed in prostatic buds. The epithelium of both canalized and uncanalized (arrow) buds exhibited nuclear labelling. Exposure period: 3 weeks; X 820

Fig. 15. Autoradiogramme of 4-week old rat ventral prostate incubated with [<sup>3</sup>H]testosterone. [<sup>3</sup>H]testosterone binding was heavy over the nuclei of prostatic epithelium, while the intensity of labelling the mesenchyme surrounding the epithelium became weaker (arrows). Exposure period: 4 weeks; X 820

Fig. 16. Autoradiogramme of 12-week old rat ventral prostate incubated with [<sup>3</sup>H]testosterone. The labelling pattern was similar to that of 4-week old prostate. Exposure period: 3 weeks; X 820



# PLATE 6



Explanation of PLATE 7 (1)

Abbreviations in figures

E, prostatic epithelium; B, prostatic bud; M, mesenchyme

Fig. 17. Histochemistry of acid phosphatase in 6-day old rat ventral prostate. No activity could be detected in the epithelial bud and mesenchyme. X 820

Fig. 18. Histochemistry of non-specific esterase in 6-day old rat ventral prostate. No activity could be detected in the epithelial bud and mesenchyme. X 820.

Fig. 19. Histochemistry of acid phosphatase in 10-day old rat ventral prostate. The epithelium of a canalized bud became positive for the activity, while that of uncanalized bud (allow ) remained negative. The black granules in the photograph represent the enzyme-actitve sites. X 820

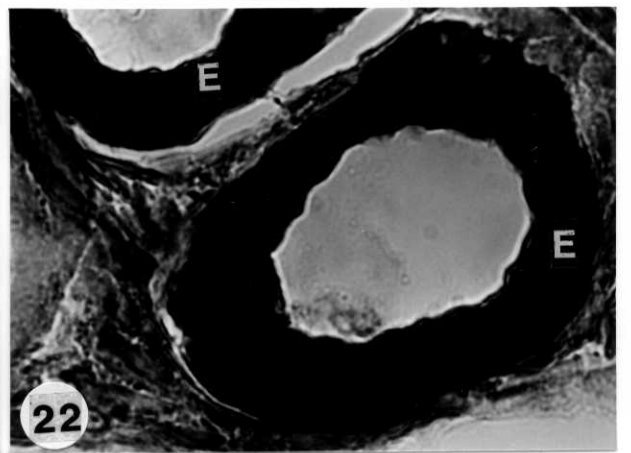
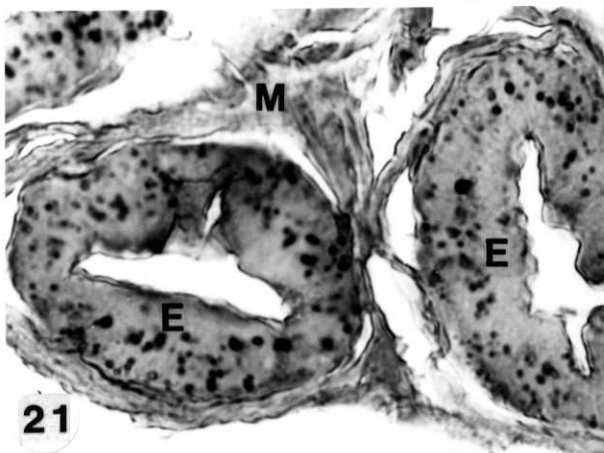
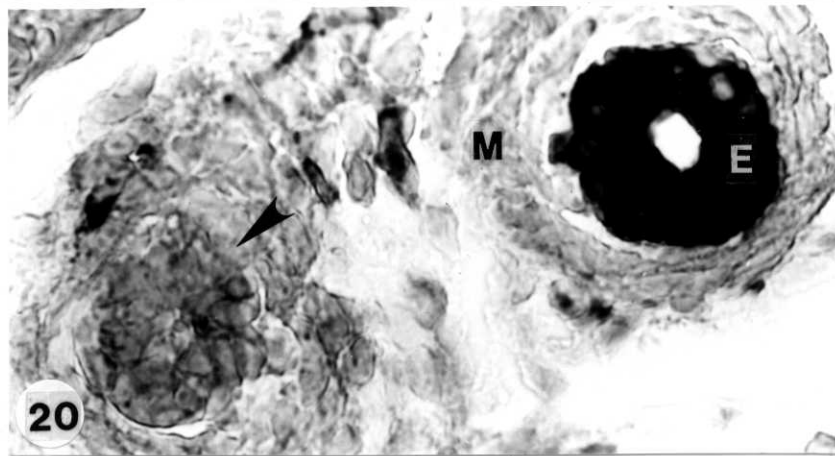
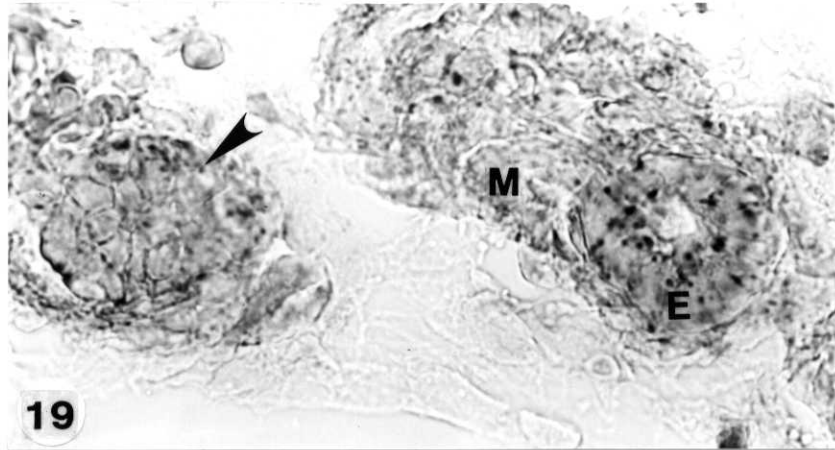
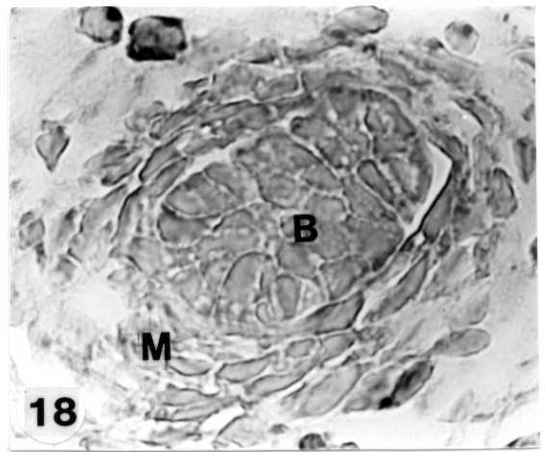
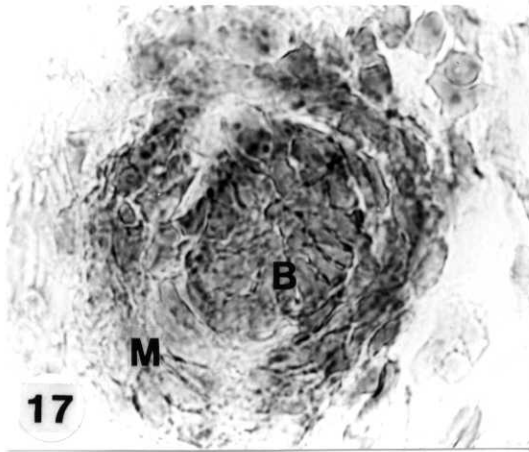
Fig. 20. Histochemistry of non-specific esterase in 10-day old rat ventral prostate. The epithelium of canalized buds became positive for the activity, while that of uncanalized (arrow) buds remained negative. The enzyme-actitve sites are black in the photograph. X 820

Explanation of PLATE 7 (2)

Fig. 21. Histochemistry of acid phosphatase in 14-day old rat ventral prostate. The epithelium was positive for the activity, while the mesenchyme remained negative. X 820

Fig. 22. Histochemistry of non-specific esterase in 14-day old rat ventral prostate. The epithelium was positive for the activity, while the mesenchyme remained negative. X 820

# PLATE 7



Explanation of PLATE 8 (1)

Abbreviations in figures

E, prostatic epithelium; M, mesenchyme

Fig. 23. Histochemistry of acid phosphatase in a recombine of Tfm mouse epithelium and rat mesenchyme. The Tfm epithelium formed prostate-like acinus. The apical part of the epithelial cells (arrow) was positive for the activity. X 550

Fig. 24. Histochemistry of acid phosphatase in a recombine of wild-type mouse epithelium and rat mesenchyme. The apical and basal part of the epithelial cells (arrows) were positive for the activity. X 550

Fig. 25. Histochemistry of non-specific esterase in a recombine of Tfm mouse epithelium and rat mesenchyme. The Tfm epithelium was positive for the activity. X 550

Fig. 26. Histochemistry of non-specific esterase in a recombine of wild-type mouse epithelium and rat mesenchyme. The epithelium was positive for the activity. X 550

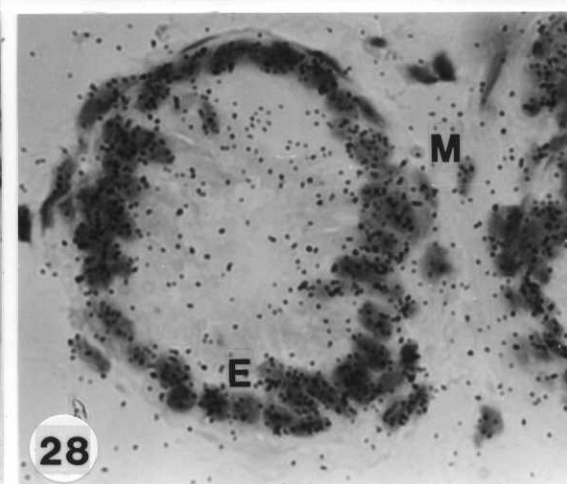
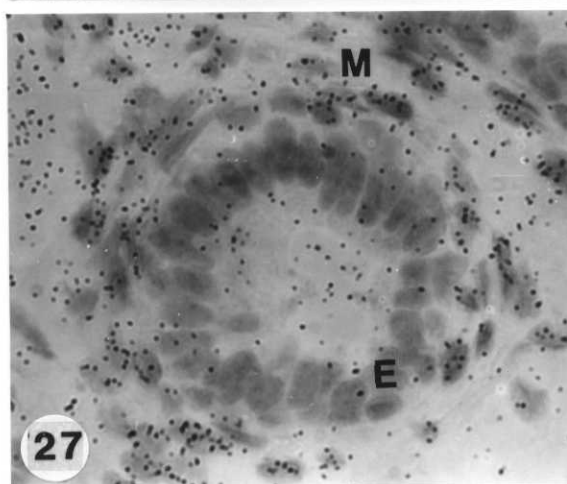
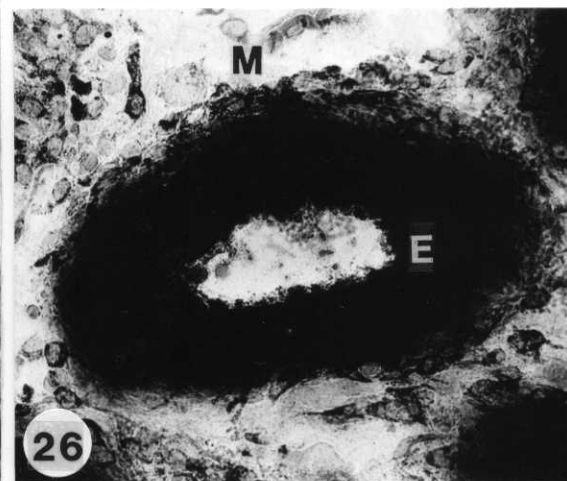
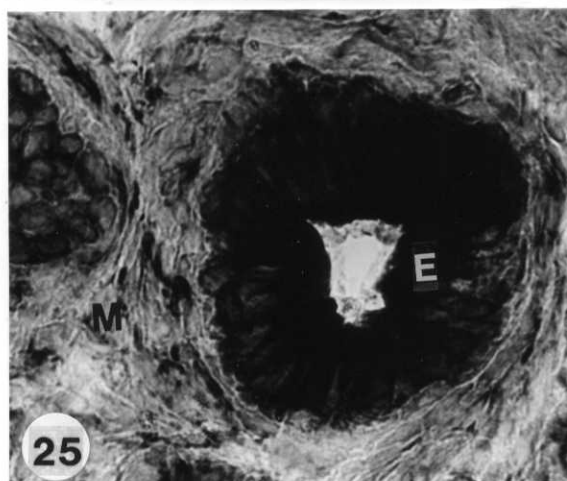
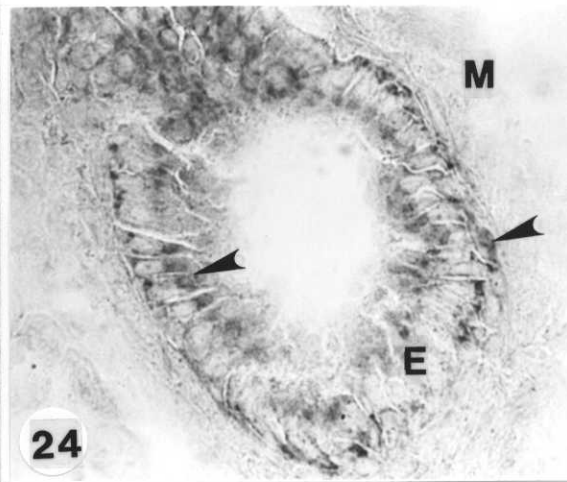
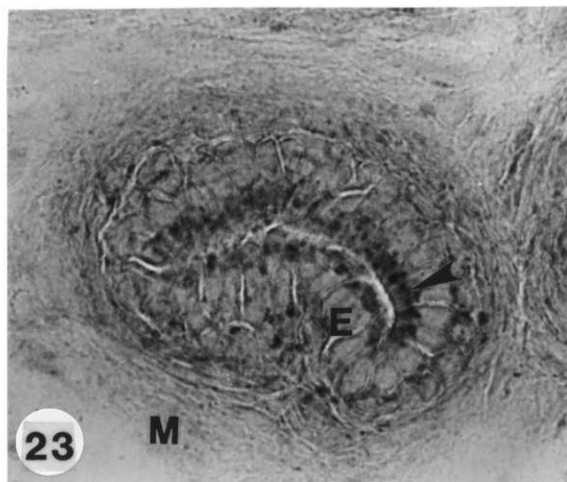
Explanation of PLATE 8 (2)

Fig. 27. Autoradiogramme of a recombinant of Tfm mouse epithelium and rat mesenchyme. The recombinant was incubated with [<sup>3</sup>H]testosterone after cultivation under kidney capsule. The epithelium showed no nuclear labelling, while the mesenchyme was labelled. Exposure period: 3 weeks; X 550

Fig. 28. Autoradiogramme of a recombinant of wild-type mouse epithelium and rat mesenchyme. The recombinant was incubated with [<sup>3</sup>H]testosterone. Both epithelium and mesenchyme were labelled. Exposure period: 3 weeks; X 550

All recombinates were grown for 4 weeks beneath the kidney capsules of male hosts.

# PLATE 8



## Discussion

The autoradiographic study presented here demonstrates the presence of androgen-binding sites in the urogenital mesenchyme. The finding supports the concept proposed in earlier work (Cunha and Lung, 1978; Lasnitzki and Mizuno, 1980a) that the mesenchyme is the target for androgens during the morphogenesis of the prostate gland. The preferential localization of sex hormones in the mesenchyme has also been demonstrated for androgen-binding sites in the fetal mouse mammary gland (Chuha, Shannon, Neubauer et al. 1981; Heuberger, Fitzka, Wasner and Kratochwil, 1982) and for estrogen-binding sites in the fetal mouse mammary gland (Stumpf, Narbaitz and Sar, 1980) and in the postnatal mouse genital tract (Cunha, Shannon, Vanderslice et al., 1982). Thus, it appears that during the phase of sexual development sex hormones exert their morphogenetic effects on the epithelium through the mesenchyme.

It is possible that the androgens act on the urogenital mesenchyme first and then result in increased epithelial proliferation and prostatic bud formation. This concept is supported by two studies. Alkaline phosphatase activity of the mesenchyme was raised by androgens and its localization was identical to that of the androgen-binding sites (Shiojiri and Mizuno, 1981), and urogenital mesenchyme associated with its epithelium greatly stimulated epithelial mitosis in the presence of androgens (Lasnitzki and Mizuno,



1979). Nuclear labelling of the mesenchyme was absent at 14.5 days but could be seen at 16.5 days of gestation. It is interesting that the time of appearance of the receptor sites coincided with or closely followed the onset of androgen secretion by the fetal testis (Picon, 1976).

In male and female sinuses a similar distribution of labelled cells was seen up to 18.5 days of gestation. At 20.5 days, however, the uptake of androgens by the mesenchyme surrounding the ventral epithelium of the female sinuses was greatly reduced. The failure of the older female sinuses to form prostatic buds (Lasnitzki and Mizuno, 1976 and 1979) may be due to such a decline in androgen receptor levels. It is not certain whether the reduction is due to a decline of receptors in all mesenchymal cells or to a migration of androgen-binding cells during the development of the vagina.

The competition experiments showed that an excess of oestradiol diminished the uptake of androgens in the sinus mesenchyme. Earlier work (Lasnitzki and Mizuno, 1980b) has shown that oestradiol combined with androgens competitively inhibits bud formation in urogenital sinuses in vitro and the present results suggest that this was due to a reduction of androgen binding. It is unlikely that this reduction is due to the aromatization of [<sup>3</sup>H]testosterone to [<sup>3</sup>H]oestradiol. Although low aromatase activity has been found in brain tissue (Naftolin, Ryan, Davies et al. 1975; Schindler, 1975), no such activity has been detected in prostatic tissue (Perel and Killinger, 1983). That

oestradiol is an effective inhibitor of androgen binding has been demonstrated for many organs: rat ventral prostate (Blondeau, Corpechot, Le Goascogne et al., 1975; Delettré, Morron, Lepicard et al., 1980), rat seminal vesicle (Zákar and Tóth, 1982), mouse kidney (Bullock and Bardin, 1974) and mouse mammary gland (Wasner, Hennermann and Kratochwil, 1983). By contrast, Shannon and Chuha (1983), using autoradiography, found that an excess of unlabelled oestradiol did not affect the distribution or intensity of nuclear [<sup>3</sup>H]dihydrotestosterone binding in mouse urogenital mesenchyme. This discrepancy may be explained by the fact that prostatic androgen receptors have a higher affinity for dihydrotestosterone than for testosterone (Mainwaring, 1969).

The incorporation of androgens into the prostatic epithelium appeared to begin immediately before the lumen formation within buds and the appearance of the acid phosphatase and non-specific esterase activities in the epithelium, and these results lead us to assume that the androgens in epithelium would play an important role in its functional differentiation. However, this assumption does not explain the results of the recombination experiments with Tfm epithelium that the prostate-like morphology and the activities of the two enzymes in the epithelium could be generated in the absence of epithelial androgen receptors. Moreover, Hironaka (in personal communication) has demonstrated by electron microscopic observation that the

fine structure of a Tfm epithelial cell of prostate-like acini induced by wild-type mesenchyme resembles that of a prostatic secretory cell containing arrays of rough endoplasmic reticulum, Golgi and secretory granules. These observations suggest that the prostatic morphology and function in the epithelium would be controlled to a great degree by the androgen-activated mesenchyme. Hence, the role of androgens in the prostatic epithelium still remains uncertain.

In conclusion the present autoradiographic and histochemical studies show that the uptake of androgens by the rat urogenital sinus is restricted to the mesenchyme during prostatic morphogenesis and that the androgen incorporation in the epithelium appears to precede its functional differentiation. The exact mechanisms by which the hormone-primed mesenchyme promotes epithelial morphogenesis and the role of androgens in the functional differentiation of the epithelium must be investigated in the future.

## Summary

Binding sites of [<sup>3</sup>H]testosterone and [<sup>3</sup>H]dihydrotestosterone in the rat fetal urogenital sinus and postnatal prostate were examined by steroid autoradiography.

1. Distinct nuclear incorporation of both androgens appeared between 14.5 and 16.5 days of gestation in rat fetuses.
2. Nuclear labelling in the sinus was restricted to the mesenchyme surrounding the epithelium which showed no nuclear labelling.
3. A similar distribution of labelled cells was observed in male and female sinuses up to 18.5 days of gestation. By 20.5 days of gestation, the labelling in the ventral mesenchyme of female urogenital sinuses became less intense but persists in the mesenchyme of the dorsal sinus wall from which the vagina is formed.
4. Uptake of [<sup>3</sup>H]testosterone by the prostatic bud epithelium was first seen at 10 days after birth, preceding its functional differentiation.
5. Recombination experiments of Tfm epithelium and wild-type mesenchyme revealed that the prostatic-like acini and the activities of acid phosphatase and non-specific esterase in the epithelium could be induced in the absence of epithelial androgen receptors.

The significance of these results, with respect to the role of epithelial-mesenchymal interaction in hormone-induced development, was discussed.

PART II.

ANALYSIS OF PROSTATIC BUD INDUCTION BY BRIEF ANDROGEN  
TREATMENT IN THE FETAL RAT UROGENITAL SINUS

\*\*\*\*\*

Introduction

In the PART I of the present thesis, I have demonstrated that the mesenchyme is an actual target for androgens and strongly suggested that prostatic bud formation is initiated by androgen-activated mesenchyme.

However, no precise data are available as regards the minimum requirements for androgens and whether their continuous presence is necessary to activate the mesenchyme.

In PART II of the thesis, male and female sinuses were grown in organ culture and treated for periods ranging from 4 to 72 hours with androgen and then transferred to hormone free medium. In addition, the uptake of labelled androgen was analysed by steroid autoradiography, and prostatic bud formation related <sup>to</sup> length of androgen exposure and degree of labelling.

## Materials and Methods

### Animals and Tissues

The urogenital sinuses of 16.5-day male and female fetuses of Wistar-Imamichi rats were used. At this stage, there is no morphological difference between male and female sinuses.

### Culture Method

The details of organ culture and steroid autoradiographic techniques were described in PART I. The urogenital sinuses were explanted whole by a modified Trowell's technique (Trowell, 1959; Lasnitzki, 1965). The culture medium was Medium 199 with Earle's salts (GIBCO Lab., Grand Island, NY, USA) supplemented with 10% fetal bovine serum, which contained 0.01 µg/ml testosterone (Koch-Light Lab. Ltd, Bucks). The explants were treated with testosterone either continuously for 5 days or for periods ranging from 4 to 72 hours followed by transfer to hormone free medium. Before transfer the explants were washed four times for 15 min. with Tyrode's solution supplemented with 30% fetal bovine serum to remove free testosterone. The total culture period was 5 days.

At the end of the culture period, the explants were fixed in Bouin's solution, embedded in paraffin wax and

serially sectioned. The sections were stained with haematoxylin-eosin. All sections were scanned under the light microscope for buds and the results were expressed both as the percentage of explants showing buds and as the average bud number per explant and its standard deviation. For each point, 4 to 11 sinuses were studied.

#### Labelling Procedure and Autoradiography

The explants were labelled with 2.5  $\mu\text{Ci/ml}$  of [1,2,6,7-<sup>3</sup>H]testosterone (92 Ci/mmol, Amersham PLC, Bucks, England) for periods of 4 to 36 hours. Those exposed for 36 hours were transferred to hormone free medium for another 36 hours to estimate the residual effect of the androgens. Before transfer or autoradiographic processing, the explants were thoroughly washed with Tyrode's solution to remove all traces of free radioactivity. To study the influence of cold androgens on the uptake of labelled testosterone, I added a 200 fold excess of unlabelled testosterone or 5 $\alpha$ -dihydrotestosterone (Kasei Chemicals, Tokyo, Japan) to the medium containing the labelled testosterone.

At the end of the culture period the explants were frozen in isopentan chilled by liquid nitrogen. The frozen sections, 5  $\mu\text{m}$  thick, were mounted on slides covered with photographic emulsion (NTB-3, Eastman Kodak Co., Rochester, NY, USA) following the thaw-mount autoradiographic technique by Stumpf and Sar (1975). The exposure time was 2 weeks.

In each explant, at least 100 mesenchymal cells, immediately adjacent to the ventral epithelium were randomly selected and the number of silver grains per nucleus was counted. The results were expressed as the average number of grains per nucleus and its standard deviation.



## Results

### A. Induction of prostatic buds by continuous exposure to testosterone

Prostatic buds were induced de novo in the 16.5-day male and female sinuses grown in vitro in the presence of testosterone (Fig. 34) and no buds were formed in the control medium (0 out of 10 explants for male, 0 out of 9 for female sinuses). Figure 29 shows the time-course of bud formation in sinuses cultured for up to 5 days. Prostatic buds appeared between day 2 and 3 of culture and thereafter their number increased rapidly to a maximum at 4 days. There was no significant difference between female and male sinuses.

To confirm that the mesenchyme is the target for androgen in bud development in vitro, I examined androgen binding sites in mesenchymal cells in the proximity of the newly formed buds by steroid autoradiography. Figure 35 shows that such mesenchymal cells were heavily labelled with [<sup>3</sup>H]androgen and that there was no uptake in the bud itself.

### B. Prostatic bud formation after brief exposure to androgen

The explants were exposed to androgen for periods

ranging from 4 to 72 hours, then transferred to control medium. Figure 30 shows the prostatic bud formation as a function of the duration of androgen-treatment. It required a minimum of 24 hours to induce buds in the male sinuses and 36 hours to induce them in the female sinuses (Fig. 30A). In both sinuses, the number of buds increased with the prolongation of the treatment (Fig. 30B). The comparison of the effects of brief exposure (Fig. 30B) with those seen after continuous treatment (Fig. 29B), shows that after transfer to control medium the bud number continued to rise to the same degree as that in explants exposed continuously for another 12-24 hours (Fig. 31). Then I examined the bud formation in control medium. In explants treated for 36 or 48 hours with androgen and then transferred to control medium, prostatic bud formation continued for about 12-24 hours similarly to that seen after continuous treatment and the increase in bud number in control medium ceased within 24-36 hours after cessation of androgen-treatment (Fig. 32).

### C. Incorporation of [<sup>3</sup>H]testosterone in the mesenchyme

To relate prostatic bud formation to mesenchymal androgen binding, I labelled male and female sinuses with [<sup>3</sup>H]testosterone for periods ranging from 4 to 36 hours and then transferred to control medium for another 36 hours and the incorporation of the hormone analysed by steroid autoradiography. Figure 33A and Figures 36a, b show that

the rate of incorporation rose steeply during the first 12 hours and then more slowly. During the first 12 hours' incubation the incorporation rate was significantly higher in the male sinuses than in the female ones. After transfer to control medium, the amount of labelled androgen concentrated in the mesenchyme, rapidly decreased within 24 hours (Fig. 33B; Fig. 36c). In the competition experiments, a 200-fold excess of cold testosterone or dihydrotestosterone in the labelling medium greatly reduced the nuclear labelling with [<sup>3</sup>H]testosterone (Fig. 33A; Fig. 36d).

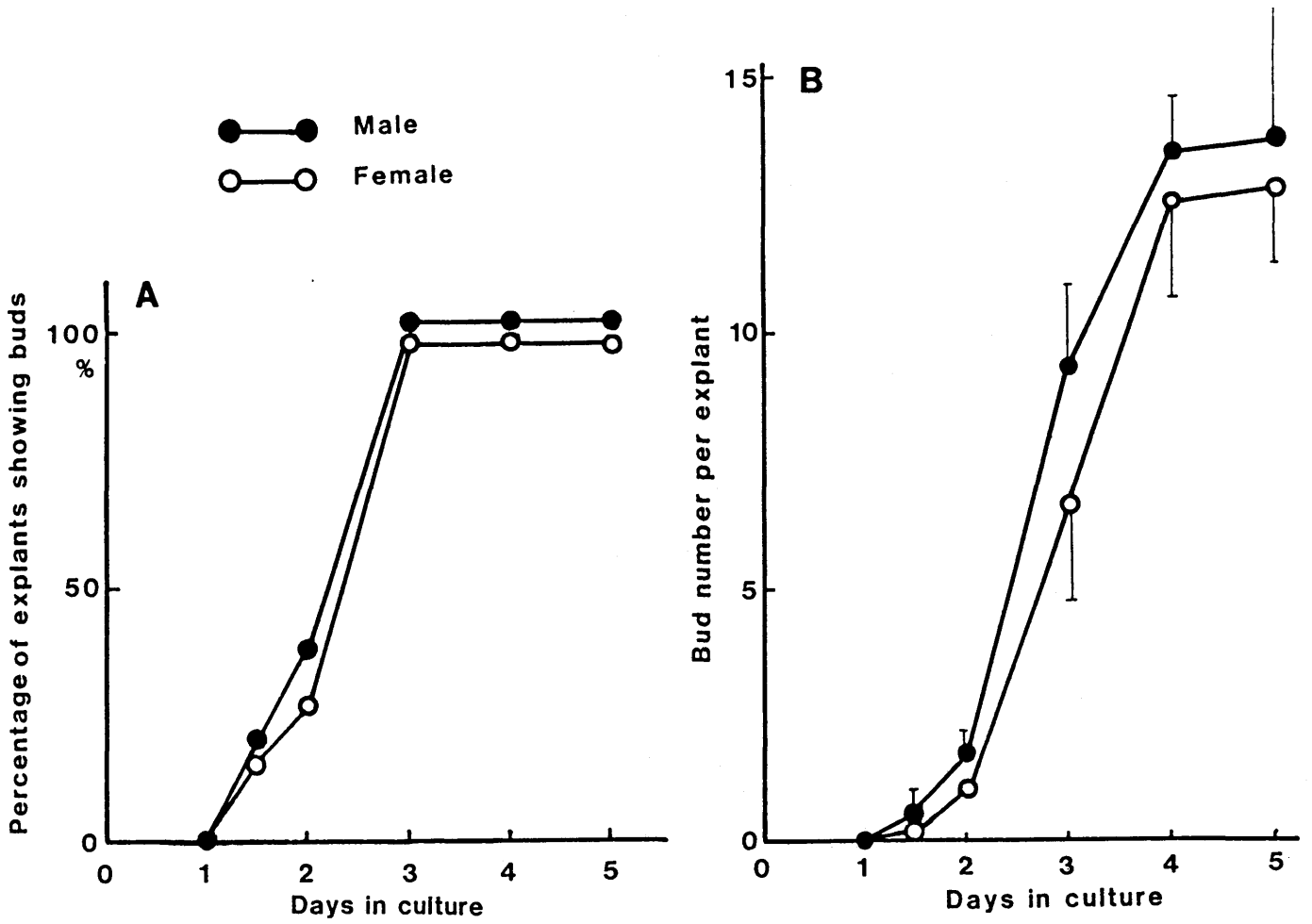


Fig. 29. Prostatic bud formation in 16.5-day male (solid circle) and female (open circle) urogenital sinuses cultured for 5 days, giving the percentage of explants showing buds (A) and the average bud number per explant and its standard deviation (B).

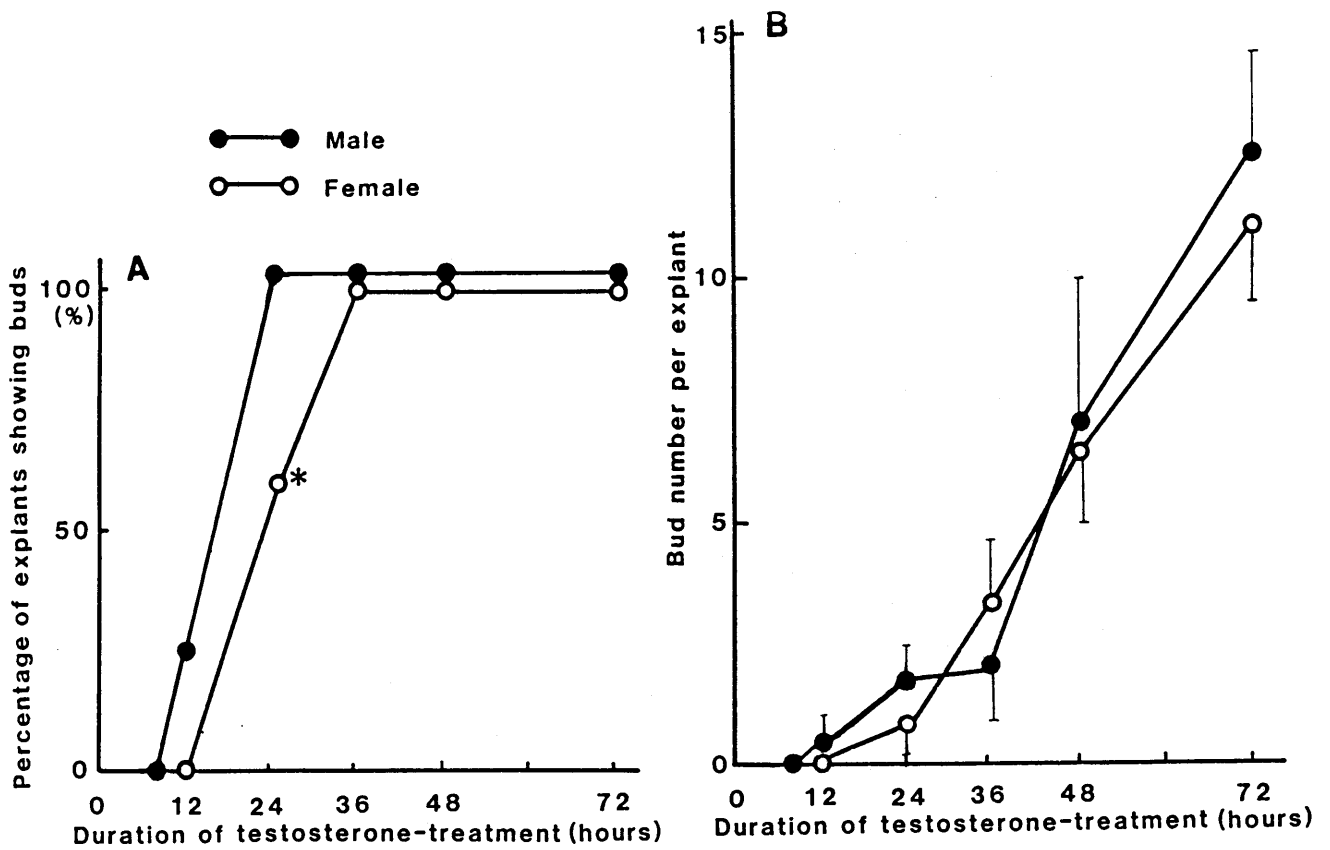


Fig. 30. Effect of brief treatments with testosterone on the bud formation of 16.5-day male (solid circle) and female (open circle) sinuses expressed as the percentage of explants showing buds (A) and the average bud number per explant and its standard deviation (B). The explants were exposed to testosterone for periods of 4, 8, 12, 24, 36, 48 and 72 hours and then transferred to control medium. The total culture period was 5 days including the period of testosterone treatment. \* denotes a significantly smaller effect in female sinuses than in male sinuses (t-Test,  $P < 0.05$ ).

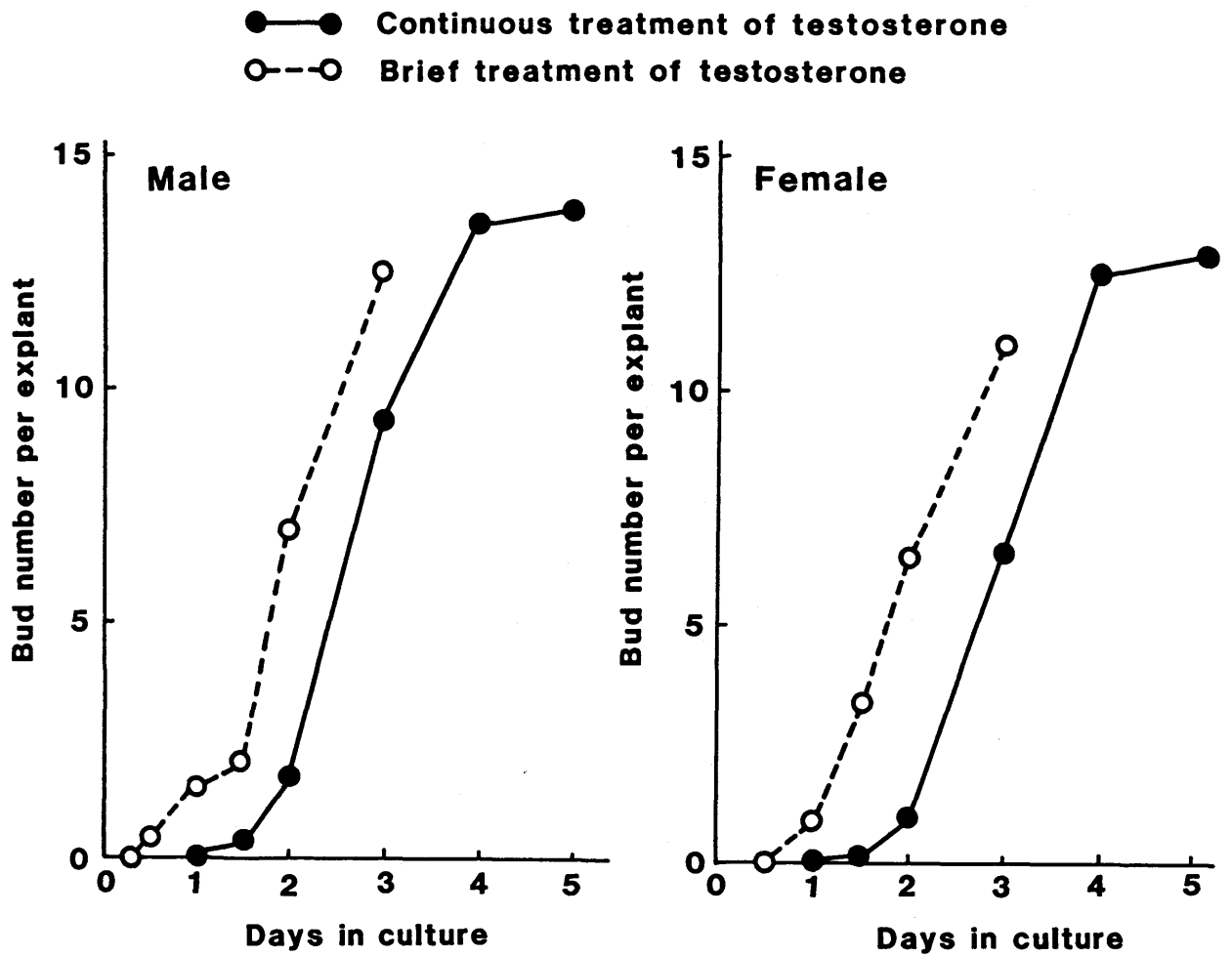


Fig. 31. Comparison between continuous (solid circle; Data from Fig. 29B) and brief treatment (open circle; Data from Fig. 30B). The abscissa represents the cultivation period for the continuous treatment and the duration of testosterone-treatment for the brief exposure experiments.

- Continuous treatment of testosterone
- - -○ 2 days' treatment followed by 3 days' culture in control medium
- △- - -△ 1.5 days' treatment followed by 3.5 days' culture in control medium

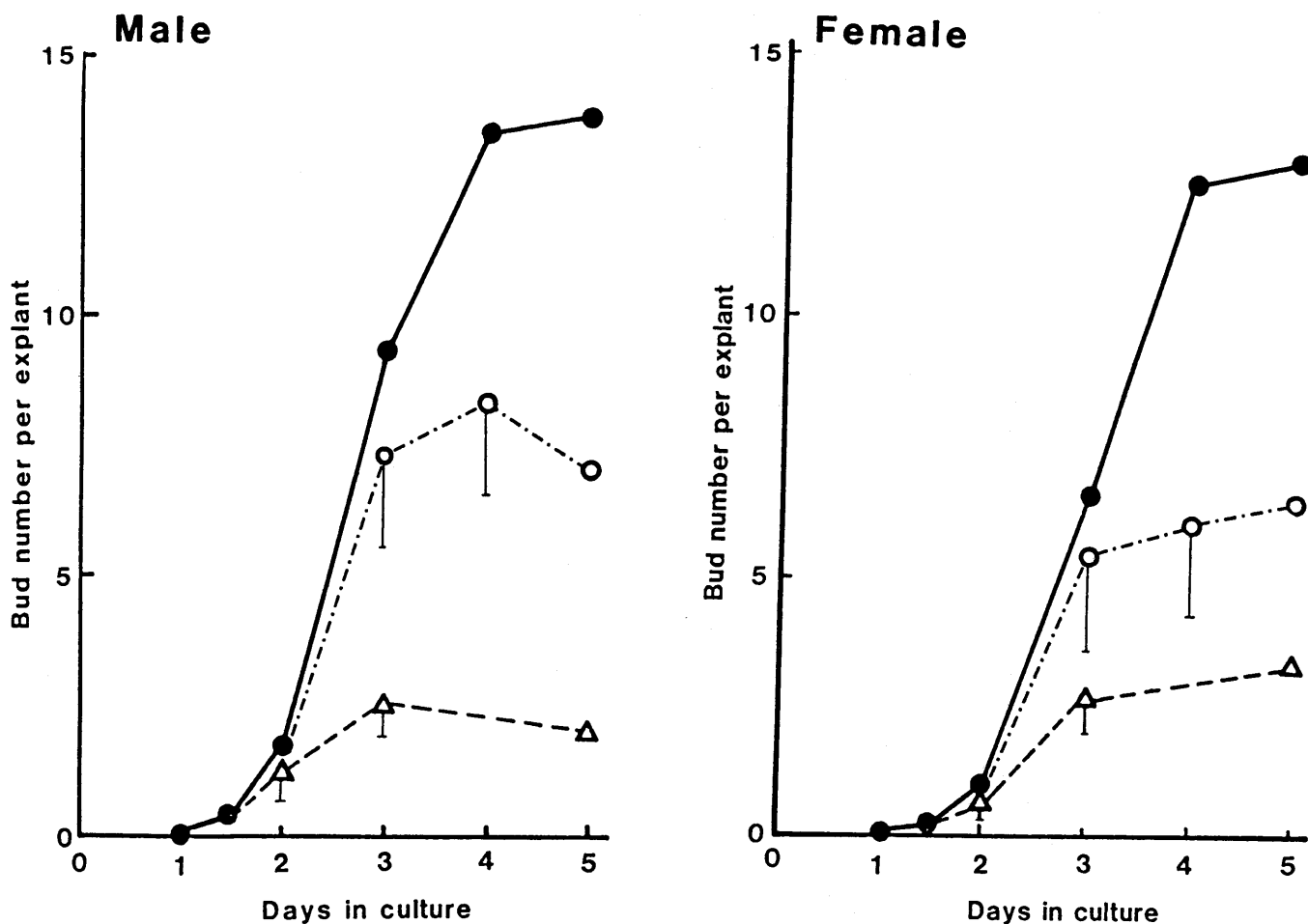


Fig. 32. Prostatic bud formation in male and female urogenital sinuses treated continuously with testosterone for 5 days (solid circle) and those treated for 2 days followed by 3 days' culture in control medium and for 1.5 days followed by 3.5 days' culture in control medium (open circle and open triangle respectively). The results are expressed as average bud number per explant and its standard deviation. In both cases the bud number increases to the same degree during the next 12-24 hours in control medium as in sinuses treated continuously, but then levels out.

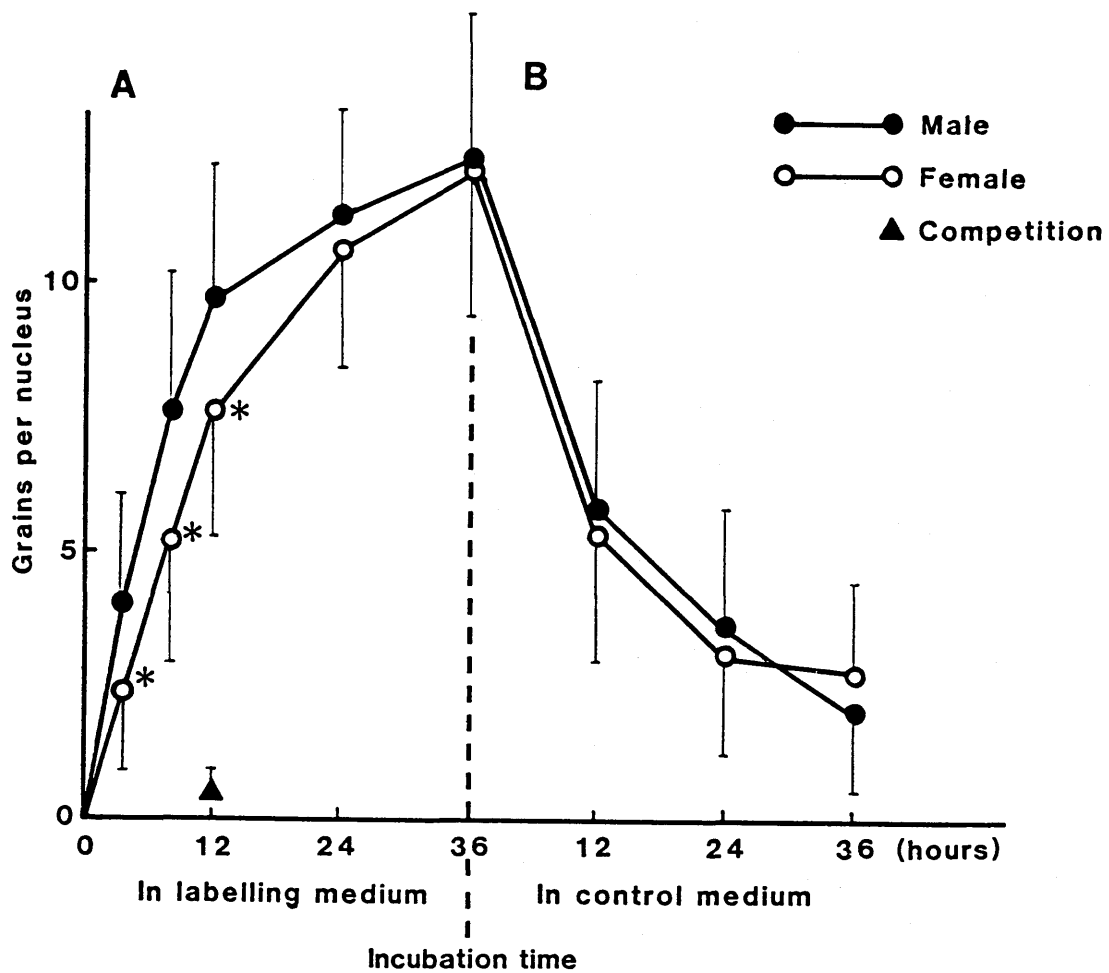


Fig. 33. (A) Incorporation of [ $^3\text{H}$ ]testosterone by 16.5-day male (solid circle) and female (open circle) sinus mesenchyme expressed as average number of silver grains per nucleus and its standard deviation. Solid triangle indicates the competition experiments with a 200 fold excess of unlabelled testosterone. At each point, more than 400 cells were randomly selected from 4 explants. \* denotes significant difference in uptake between male female sinuses (t-test,  $P < 0.05$ ). (B) Residual label in the sinuses transferred to control medium after 36 hours' incubation with [ $^3\text{H}$ ]testosterone. At each point, more than 300 cells randomly selected from 3 explants were counted.



Explanation of PLATE 9

Abbreviations in figures

B, prostatic bud; E, epithelium

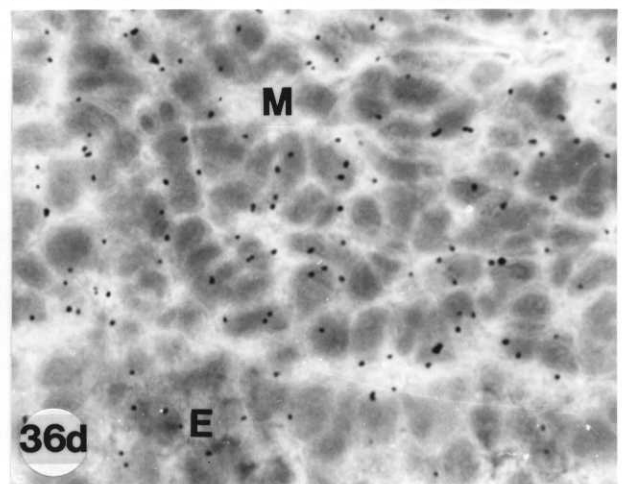
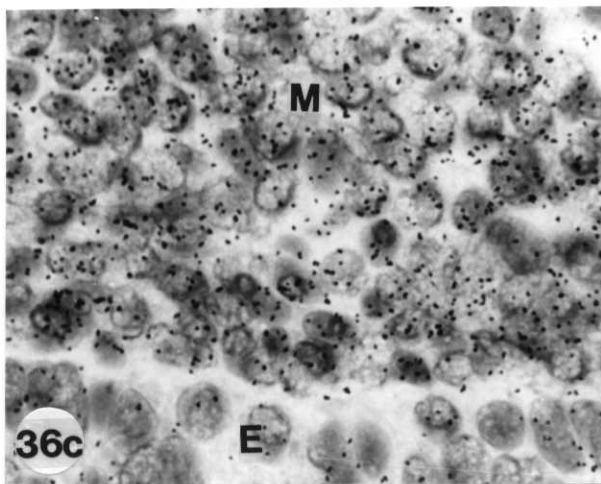
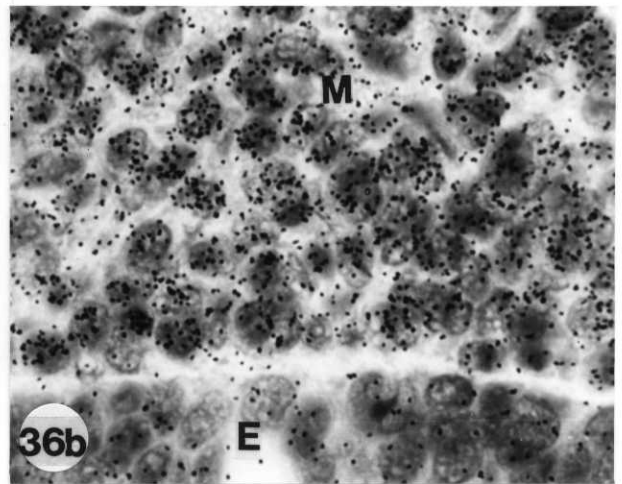
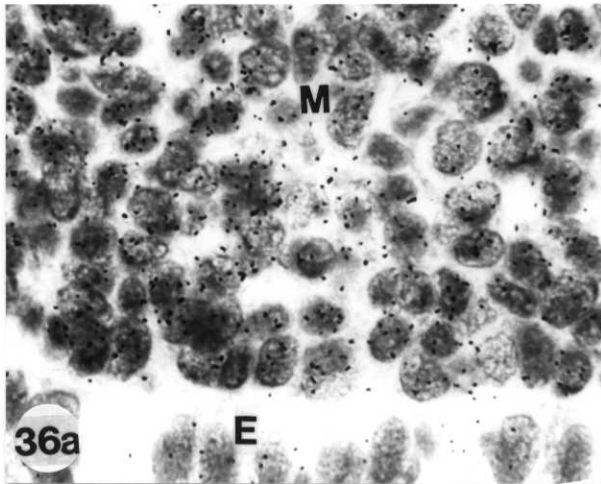
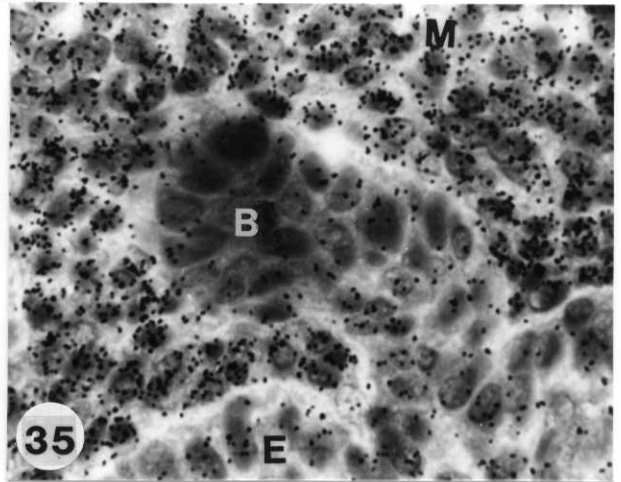
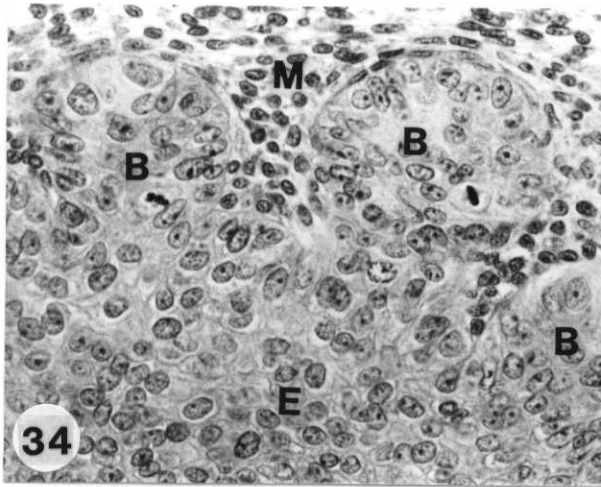
M, mesenchyme.

Fig. 34. Urogenital sinus of 16.5-day male fetus exposed in vitro for 3 days to testosterone showing prostatic buds. X 460

Fig. 35. Autoradiogramme of an area close to an induced bud. The male sinus was exposed to unlabelled testosterone for 2 days, transferred to the control medium for 1 day to remove cold hormone and then incubated with [<sup>3</sup>H]testosterone for 12 hours. Note heavy labelling of mesenchymal cells close to the epithelial bud. Exposure period: 3 weeks; X 700

Figs. 36. Autoradiogrammes of urogenital sinuses of 16.5-day female fetuses. (a) 4 hours' incubation with [<sup>3</sup>H]testosterone showing weak labelling, (b) 12 hours' incubation with [<sup>3</sup>H]testosterone showing heavy labelling, (c) 12 hours' incubation in control medium after 36 hours' exposure to [<sup>3</sup>H]testosterone showing weak labelling, (d) 12 hours' incubation with [<sup>3</sup>H]testosterone in the presence of a 200 fold excess of unlabelled dihydrotestosterone. Labelling was absent. Exposure period: 2 weeks; X 750

# PLATE 9



## Discussion

The results confirm that androgens induce prostatic buds de novo in urogenital sinuses in organ culture and that the androgen-primed mesenchyme promotes epithelial bud formation. The studies on brief treatment of androgen show that a minimum of 24 hours' exposure to testosterone is necessary to induce buds in the male sinuses and 36 hours' in female sinuses. In both sexes the number of prostatic buds increases with length of exposure and rises further for 24-36 hours after cessation of androgen treatment. Testosterone incorporation into the mesenchymal nuclei also increases with length of exposure to the hormone but is greatly reduced within 24 hours following the end of exposure. This fall of labelled hormones in the mesenchyme is followed by a corresponding fall in bud formation. In consideration of the lag-period necessary for the epithelial-mesenchymal interaction, it is reasonable to say that the prostatic bud formation in the sinus of 16.5-day fetuses is quite androgen-dependent: the mesenchyme does not induce the epithelial buds unless the mesenchymal cells incorporate a certain amount of androgens in their nuclei and the mesenchyme lose the bud-inducing ability just after the loss of androgens.

A comparison of the incorporation rates of male and that of female sinuses shows that they were significantly lower in female sinuses than those in male ones during the first 12

hours. This result explains why the longer period of androgen-treatment was required for female sinuses to induce buds and again confirms the relationship between mesenchymal androgen incorporation and bud induction. According to Boesel, Klipper and Shain (1980) and Blondeau, Baulieu and Robel (1982), androgens increase receptor levels in target tissues. Rat fetal testes begin to secrete androgens at 15 days of gestation (Warren, Haltmeyer and Eik-Nes, 1973; Lasnitzki and Mizuno, 1977) and it is possible that the endogeneous exposure to androgens before explantation has raised the receptor level in the male sinuses beyond that of the female sinuses. However, it is worth noting that sexual differences existed only in the early phase of incubation and that they became less remarkable with prolongation of androgen-exposure. This suggests that 16.5-day female urogenital sinuses possess essentially the same activity as male ones with respect to androgen incorporation and bud formation.

In conclusion, the present investigation reveals that the continuous presence of androgen is necessary to activate the mesenchyme and that the sexual difference as regards androgen incorporation and bud induction already exists in the young sinus though they show no morphological differences yet.

## Summary

The androgen dependency of prostatic bud formation in fetal rat urogenital sinuses was studied using brief treatments with androgen. 16.5-day fetal sinuses of both sexes were grown in organ culture and treated with androgens for periods ranging from 4 to 72 hours and then transferred to hormone free medium. Under these conditions it required 24 hours' treatment to induce prostatic buds in all male sinuses and 36 hours in all female sinuses. The number of buds induced increased with prolongation of exposure. Prostatic bud formation continued for 24-36 hours after transfer to control medium but thereafter very few new buds appeared. Steroid autoradiographic analysis showed that the mesenchyme of male sinuses concentrated androgens more rapidly than that of female ones and that the amount of residual androgens in the mesenchyme of explants transferred to hormone free medium was greatly reduced within 24 hours. These results indicate that at least in the sinus of 16.5-day fetuses, continuous presence of androgen is necessary to activate the mesenchyme.

PART III  
BEHAVIOUR OF ANDROGEN-ACTIVATED MESENCHYMAL CELLS  
DURING PROSTATIC BUD FORMATION

\*\*\*\*\*

Introduction

In the previous parts of the present thesis, it was demonstrated that the prostatic bud formation requires the interaction of the epithelium with the androgen-activated mesenchyme. For the further studies of the mechanism of the epithelial-mesenchymal interaction, it is essential to reveal the behaviour of the mesenchymal cells at the epithelio-mesenchymal interface. However, no such attempts have been made so far because of the lack of cell marking system. During the studies, I found that X-inactivation mosaicism as to Tfm gene provided a good experimental system for analysing the behaviour of androgen-activated mesenchymal cells in the prostatic morphogenesis.

X-chromosome inactivation occurs early in the embryonic development of mammary females carrying two X-chromosomes (Lyon, 1961; Monk and Harper, 1979). It is cell autonomous and irreversible, producing X-inactivation mosaics where the maternal X-chromosome is inactive in some cells and the

paternal one in the others. Many studies have been carried out to investigate the proportion and distribution of the two cell types in X-inactivation mosaics but there were a very few genetic markers by which the two cell types could be identified at a cellular level (Mystkowska and Tarkowski, 1968; Condamine, Custer and Mintz, 1971). Since androgen-binding sites can be visualized at a cellular level by means of steroid autoradiographic technique, testicular feminization (Tfm) locus of the X-chromosome seems a suitable genetic marker for the histological examination of X-chromosome mosaicism and also for the study of androgen-dependent changes in cell behaviour.

In the present study, I visualized the distribution of androgen-receptor positive (Tfm gene inactive) and negative (Tfm gene active) cells in the sinus mesenchyme of  $X^{Tfm}/X^+$  heterozygous female mice, and examined the changes in mosaic pattern after androgen-treatment. These results could provide the useful information for the behaviour of the mesenchymal cells in the androgen-induced epithelial-mesenchymal interaction.

## Materials and Methods

### Animals and Tissues

The urogenital sinuses of 15.5-day mouse fetuses were used in this study. 15.5-day-old male ( $X^+/Y$  and  $X^{Tfm}/Y$ ) and female fetuses ( $X^{Tfm}/X^+$  and  $X^+/X^+$ ) were obtained by mating female carriers ( $X^{Tfm}/X^+$ ) with wild-type males ( $X^+/Y$ ). The identification of male fetuses ( $X^+/Y$  or  $X^{Tfm}/Y$ ) was carried out by histological examination of mammary gland rudiments (See Figs. 4). All fetuses were handled individually.

### Labelling procedures and Autoradiography

The labelling and steroid autoradiography were done in the same way as described in PART I except the exposure period. The exposure period was prolonged to 2 months, which allowed me to identify with much reliability the two cell types; labelled (Tfm gene inactive) and unlabelled (Tfm gene active) cells. The nuclei possessing more than 15 silver grains were considered androgen-receptor positive.

### Statistical analysis

In the urogenital mesenchyme of  $X^{Tfm}/X^+$  fetuses, the coherent clone size was estimated by the method of West (1975 and 1976b). The mean coherent clone length was



estimated by dividing the observed mean patch length by  $1/(1-p)$ , where  $p$  is the proportion of each cell type (West, 1975). For each animal, 4 to 5 sections were selected and the observed patch lengths were measured along a random line across the photograph of the section (6-8 random lines in each section) (See the legend for Table 3).

#### Androgen-treatment and Autoradiography

Figure 37 gives the experimental design used for the present study.

Urogenital sinuses were cultured in vitro for 4 days in the presence of 0.01  $\mu\text{g/ml}$  testosterone and were examined histologically for the appearance of buds and the number of induced buds. To identify two types of female fetuses ( $X^+/X^+$  or  $X^{\text{Tfm}}/X^+$ ), I isolated the urethra just near the sinus, immediately labelled it with [ $^3\text{H}$ ]testosterone for 12 hours, and determined the proportion of labelled and unlabelled cells in its mesenchyme.

For steroid autoradiographic analysis, the urogenital sinus was separated into two parts. One was immediately subjected to steroid autoradiography to examine the mosaic pattern before androgen-treatment (I call this androgen-untreated fragments of the sinus in the following). The other was exposed to testosterone (0.01  $\mu\text{g/ml}$ ) for 1 or 2 days, then cultured in hormone-free medium for 1 or 2 days respectively to reduce the androgen incorporated into the

**A. Prostatic bud induction  
in mosaic sinuses**

**B. Steroid autoradiographic analysis**

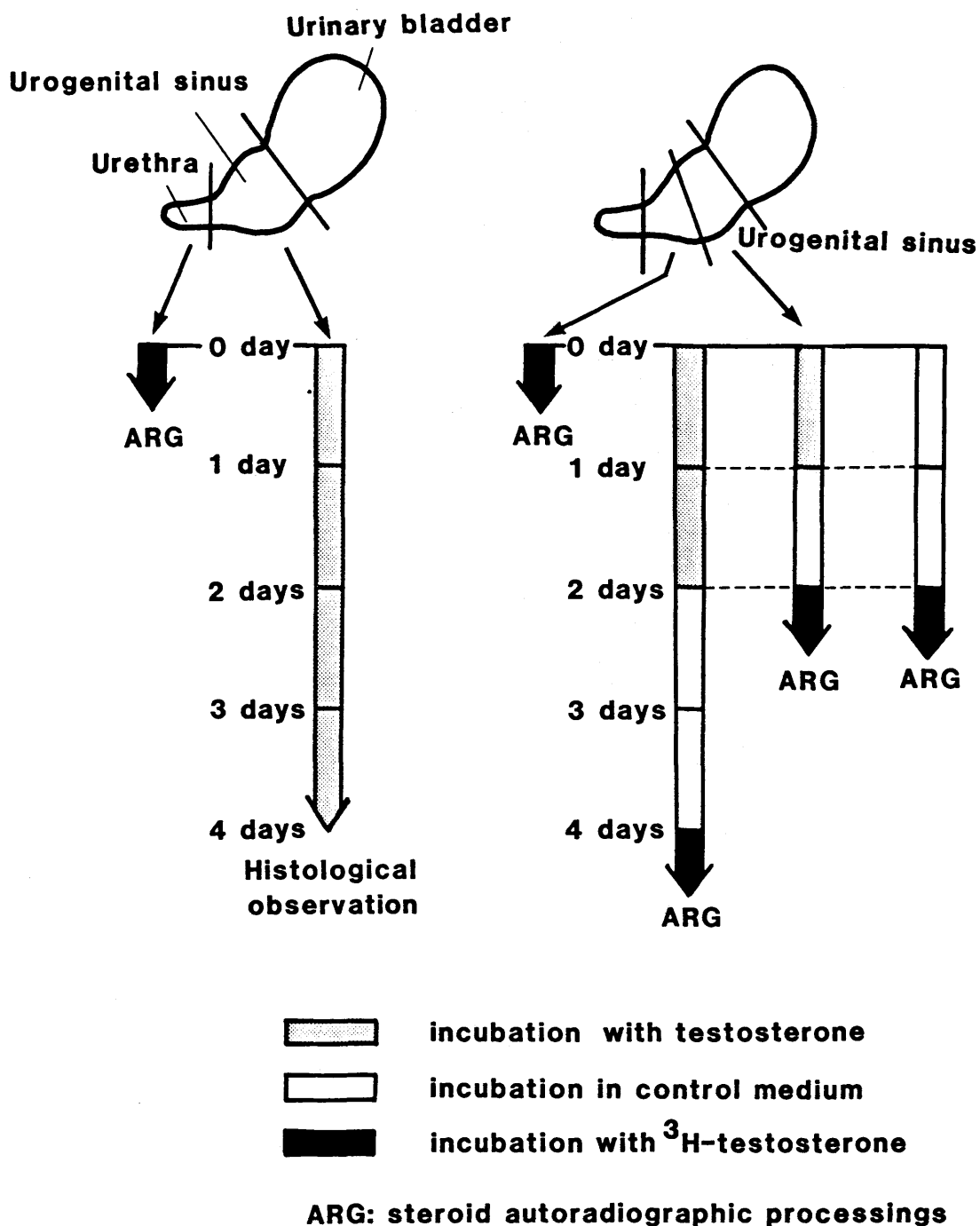


Fig. 37. Experimental design used for the present study.

mesenchyme, which could compete with [<sup>3</sup>H]testosterone, and were labelled with [<sup>3</sup>H]testosterone for 12 hours followed by steroid autoradiographic processings. As a control I examined the urogenital sinuses which were cultured in androgen-free medium for 2 days and were processed for steroid autoradiography. The average number of silver grains over the nuclei in the autoradiogrammes of androgen-treated explants was reduced to about a half as compared with that of androgen-untreated ones. This might be due to the influence of the low level of residual unlabelled androgens. Therefore, the exposure period was further prolonged to 3 months and the nuclei possessing more than 7 grains were considered androgen-receptor positive cells.

#### Labelling Index

At the end of culture, [methyl-<sup>3</sup>H]thymidine (52 Ci/mmol, Amersham) was added to the culture medium at a concentration of 10  $\mu$ Ci/ml and the explants incubated for 4 hours. After labelling they were fixed in Carnoy's solution for 1 hour, washed in three changes of absolute ethanol, embedded in paraffin wax and serially sectioned. After Feulgen staining, the mounted sections were coated with Kodak NTB-3 emulsion by the dipping technique. After 5 days' exposure in the dark at 4°C, the slides were developed and fixed as described in steroid autoradiographic technique. The nuclei possessing more than 10 silver grains was considered labelled cells.

## Results

### Chapter 1. Visualization of X-chromosome mosaicism in testicular feminization mutant mice

I first examined 15.5-day male urogenital sinuses of wild-type male ( $X^+/Y$ ) and Tfm mutant male ( $X^{Tfm}/Y$ ) mice. In urogenital mesenchyme of wild-type mice almost all cells showed nuclear labelling while no labelling in the Tfm mutant mesenchyme (Figs. 38a and b). These results show that Tfm mutant cells can be distinguished from wild-type ones in autoradiogrammes.

There were no additional markers which identify the two genotypes of female mice ( $X^+/X^+$  and  $X^{Tfm}/X^+$ ) in embryonic stages. However, I could find the two distinct populations of female mesenchymes as to the proportion of labelled and unlabelled cells: one is that almost all mesenchymal cells were labelled as in wild-type male mesenchyme ( $X^+/Y$ ) and the other is that only about a half of them were labelled (Table 3). From these observations it is reasonable to say that the latter population of female mesenchymes represents that of heterozygous ones ( $X^{Tfm}/X^+$ ).

In the mesenchyme of urogenital sinuses of wild-type females ( $X^+/X^+$ ), the nuclei of most cells were labelled (Fig. 39a), while in the mesenchyme derived from heterozygous females ( $X^{Tfm}/X^+$ ), labelled and unlabelled cells were present (Fig. 39b). Cell counts confirmed this observation.

Explanaion of PLATE 10

Figs. 38. a, b. Autoradiogrammes of urogenital mesenchymes of 15.5-day wild-type ( $X^+/Y$ ) and Tfm-mutant ( $X^{Tfm}/Y$ ) male fetuses respectively. Exposure period: 2 months. Almost all cells were labelled in wild-type mesenchyme (a), while none of them were labelled in Tfm mutant mesenchyme (b). X 660

Figs. 39. a, b. Autoradiogrammes of urogenital mesenchymes of 15.5-day wild type ( $X^+/X^+$ ) and heterozygous ( $X^{Tfm}/X^+$ ) female fetuses respectively. Exposure period; 2 months. Nuclei possessing more than 15 silver grains were considered to be androgen receptor-positive (i.e. Tfm gene inactive in  $X^{Tfm}/X^+$  target tissues). Androgen-incorporating cells were present in the urogenital mesenchyme surrounding the epithelium. More than 95% cells in  $X^+/X^+$  mesenchyme were receptor-positive (a), while about 50% cells in  $X^{Tfm}/X^+$  mesenchyme showed no nuclear labelling (Tfm-gene active) (b). X 650

Figs. 40. a, b. Autoradiogrammes of mammary glands of 15.5-day wild type ( $X^+/X^+$ ) and heterozygous ( $X^{Tfm}/X^+$ ) female fetuses respectively. Exposure period: 1 month. In  $X^+/X^+$  fetuses almost all mesenchymal cells existing in 2-4 layers beneath the mammary bud epithelium (E) were receptor-positive (a), while in  $X^{Tfm}/X^+$  fetuses a large number of receptor-negative cells were present in the close proximity of the mammary bud epithelium and receptor-positive and receptor-negative cells coexisted forming small clusters (b). X 270

# PLATE 10

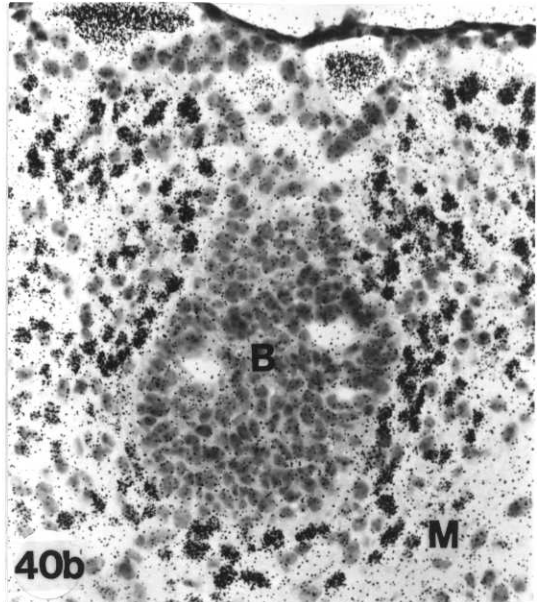
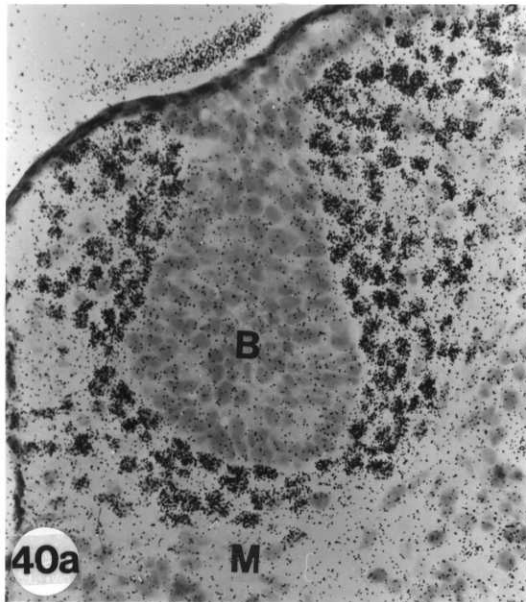
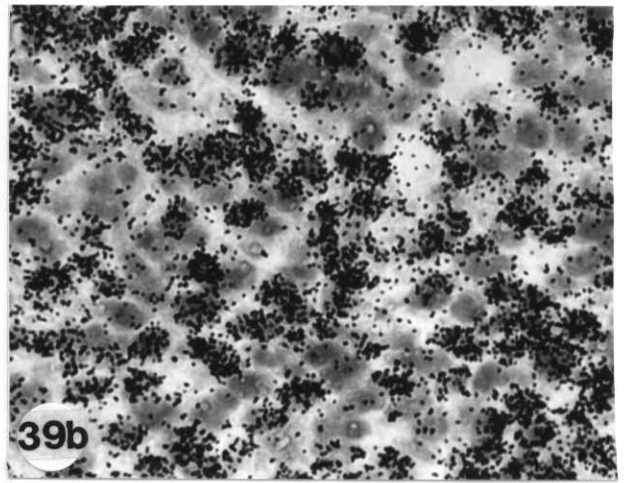
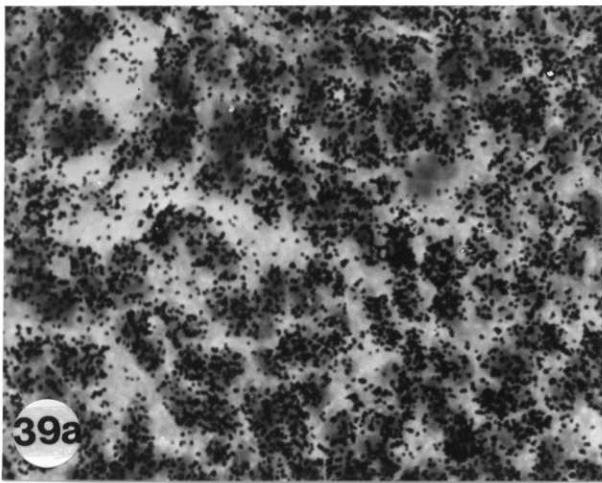
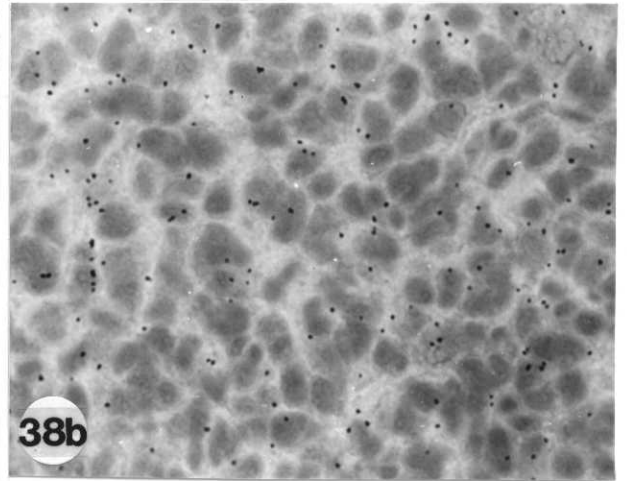
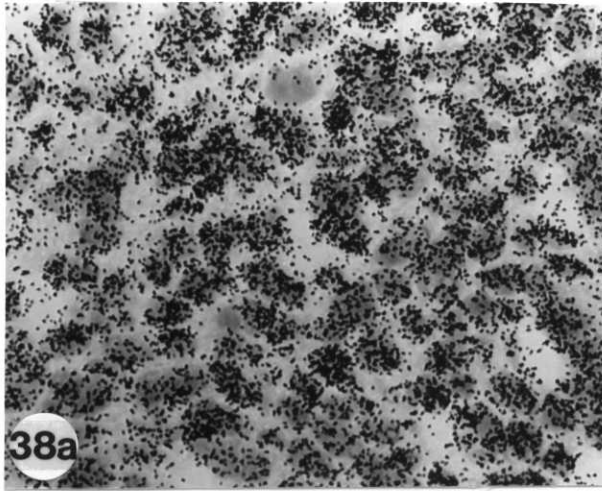


Table 3. Statistical analysis of coherent clone size in urogenital sinuses of  $X^{Tfm}/X^+$  female fetuses

Animal No.	Mean Proportion of Receptor-Positive Cells (p x 100) (%)	*b Mean observed Patch Length $L_{patch}$ ( $\mu m$ )	*c Mean Estimated Coherent clone Length ( $\mu m$ ) $L_{coher} = L_{patch} (1-p)$	*d No. of Nuclei per clone $N = (L_{coher})^3 D_N$
I. Cross Section: *e Mean Nuclear Density ( $D_N$ ) = $1.4 \times 10^{-3} \mu m^{-3}$				
2171	44.4 *a	20.9	11.6	2.1
2188	51.8	24.8	11.9	2.3
2191	56.2	29.3	13.4	3.3
2205	56.8	28.6	12.3	2.5
2208	47.0	25.2	13.3	3.2
Mean $\pm$ S. D.	51.2 $\pm$ 5.5		12.5 $\pm$ 0.8	2.7 $\pm$ 0.5
II. Sagittal Section: *e Mean Nuclear Density ( $D_N$ ) = $1.6 \times 10^{-3} \mu m^{-3}$				
2256	57.9	26.1	11.0	2.1
2259	60.8	31.1	12.1	2.8
2260	51.5	20.8	10.2	1.7
2265	31.6	18.0	12.2	2.8
Mean $\pm$ S. D.	50.4 $\pm$ 13.1		11.4 $\pm$ 1.0	2.4 $\pm$ 0.5
III. Wild Type ( $X^+/X^+$ )				
Mean $\pm$ S. D.	96.0 $\pm$ 1.0	( 5 animals)		

Legend for Table 3.

\*a Values represent the mean from 4-5 sections in each animal.

\*b Observed patch lengths ( $L_{\text{patch}}$ ) were measured along a random line across the photograph of the section (6-8 random lines in each section). The nuclei possessing more than 15 silver grains in the autoradiogram were considered to be receptor-positive.

\*c Mean coherent clone length ( $L_{\text{coher}}$ ) were estimated from the relation  $L_{\text{coher}} = L_{\text{patch}} / L_{\text{random}}$ , where  $L_{\text{patch}}$  denotes each observed patch length and  $L_{\text{random}}$  the random clone length equal to  $1/(1-p)$  (West, 1975). The above relation  $L_{\text{patch}} = L_{\text{coher}} \cdot L_{\text{random}}$  is based on the fact that the random distribution of coherent clones accounts for the observed patch distribution.

\*d The number of nuclei per coherent clone (N) was estimated by multiplying the cube of coherent clone length,  $(L_{\text{coher}})^3$ , by the average nuclear density.

\*e The nuclear density ( $D_N$ ) was calculated according to the following equation (Abercrombie, 1946):

$$N_P = N_C \left( \frac{T}{L_N + T} \right), \quad D_N = N_P / T$$

where  $N_P$  is the average number of 'nuclear points' per section,  $N_C$  is the count of visible nuclei per section,  $T$  is the thickness of the section and  $L_N$  is the average length of the nuclei.



In the urogenital mesenchyme of wild-type females about 95% and in sinuses of mosaic mice about 50% of the cells were labelled. Thus, the Tfm gene was expressed only in a half of the sinus mesenchymal cells of heterozygous females.

In the mosaic mesenchyme labelled and unlabelled cells formed small irregular clusters. One-dimensional clonal analysis was used to estimate the coherent clone size in the urogenital mesenchyme. Table 3 shows the mean proportion of receptor-positive cells and the mean coherent clone length. The number of nuclei per coherent clone (N) was estimated by multiplying the cube of coherent clone length by the average nuclear density (see legend for Table 3). From these calculations, it was estimated that in the urogenital mesenchyme each coherent clone of receptor-positive cells consisted of 2-3 cells and there was no significant difference between cross and sagittal sections (Table 3).

The same mosaic pattern was also observed in other androgen-target tissues such as mammary gland rudiments (Figs. 40a and b).

## Chapter 2. Behaviour of androgen-incorporating cells during prostatic morphogenesis

### A. Prostatic bud formation in urogenital sinuses of heterozygous female mice ( $X^{Tfm}/X^+$ )

Female urogenital sinuses were cultured for 4 days in the presence of testosterone. The genotype of these fetuses was determined by the autoradiogramme of their urethrae of which the mesenchyme showed wild-type or mosaic pattern of labelling ( $X^+/X^+$  or  $X^{Tfm}/X^+$  respectively) (Figs. 41a and b). Prostatic buds were induced de novo in the sinuses of both genotypes, and the induced bud number in the mosaic sinuses reached to as much as 70% of that in wild-type ones (Figs. 42a and b, Table 4). Moreover, at least from the light microscopic observations, the morphology of induced buds in the mosaic sinuses was identical with that in the wild-type ones.

B. Autoradiographic analysis of the changes of mosaic pattern after androgen-treatment

I examined by steroid autoradiography the distribution of labelled and unlabelled mesenchymal cells in the proximity of induced buds in mosaic sinuses. When the female sinuses were cultured for 2 days in the presence of testosterone and then for 2 days in control medium, prostatic buds were induced in the female sinuses of both genotypes. In the wild-type sinus, labelling pattern did not differ from that in androgen-untreated fragment of the sinus: almost all mesenchymal cells were labelled (Figs. 43a and b). In the heterozygous sinuses, the mosaicism, which has been confirmed in the androgen-untreated fragment of the

Table 4. Number of Induced prostatic buds in female sinuses after 4 days' culture with testosterone

Phenotype	Genotype	No. of explants	No. of induced buds (Mean $\pm$ S.D)
Wild*1	X <sup>+</sup> / X <sup>+</sup>	14	28.0 $\pm$ 4.3
Mosaic*2	X <sup>Tfm</sup> / X <sup>+</sup>	9	18.2 $\pm$ 3.6

\*1 Wild represents fetuses where more than 90% of mesenchymal cells of their urethrae were labelled.

\*2 Mosaic represents fetuses where the proportion of labelled mesenchymal cells in their urethrae was between 40%-60%.

Explanation of PLATE 11

Abbreviations in figures

UE, urethral epithelium; UM, urethral mesenchyme;

E, sinus epithelium; M, sinus mesenchyme; MF, Millipore filter

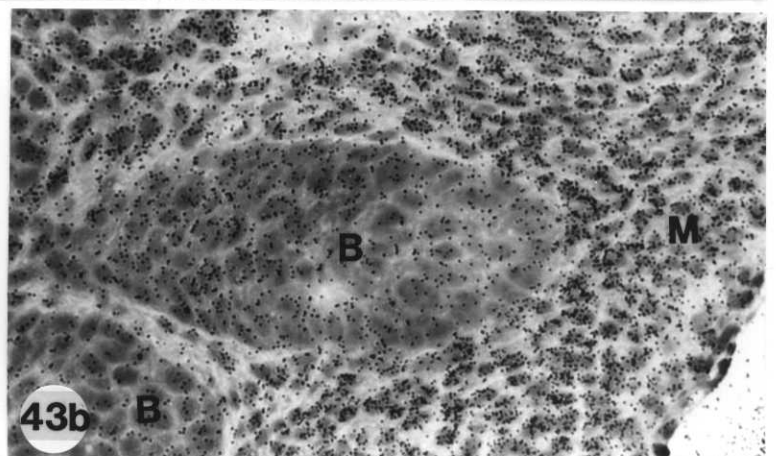
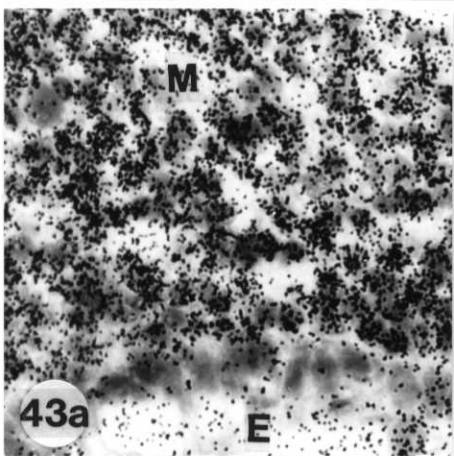
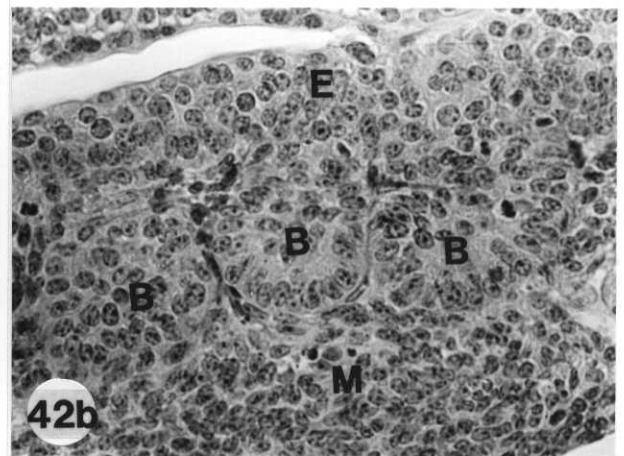
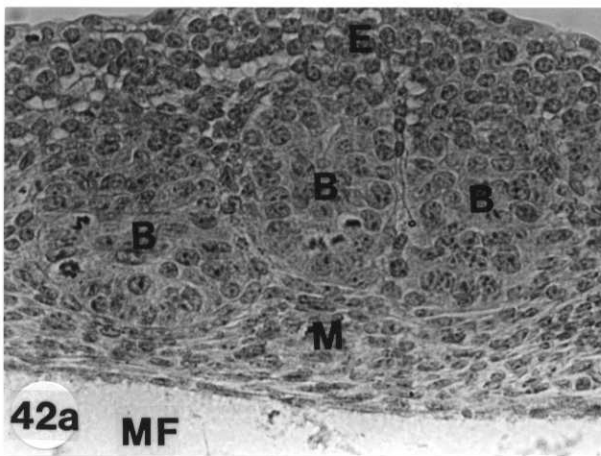
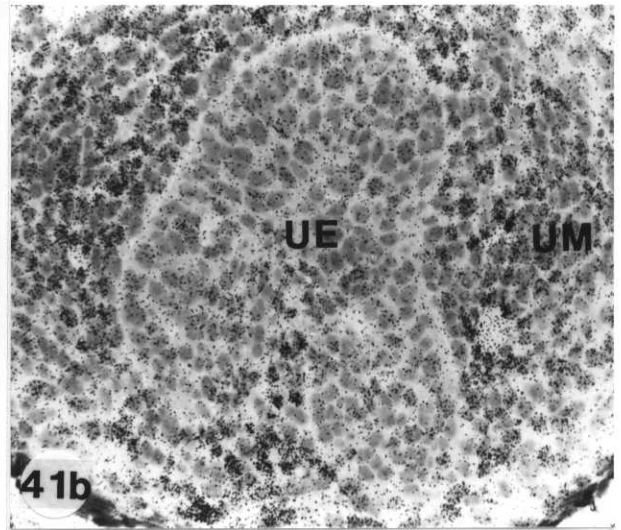
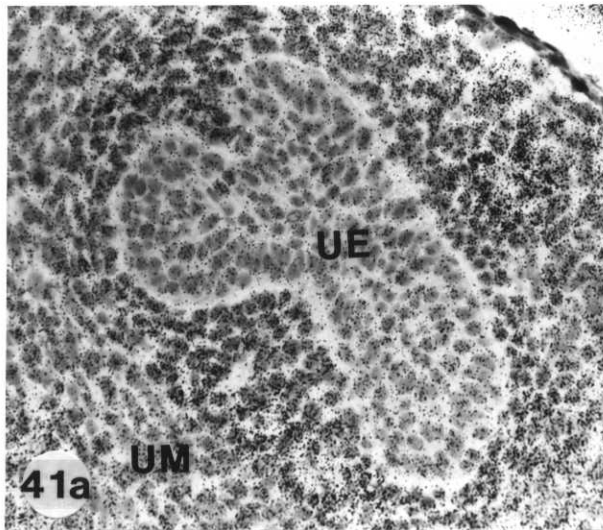
Figs. 41. Autoradiogrammes of wild-type (a) and mosaic (b) urethrae. In the mesenchyme of wild-type urethra almost all cells were labelled while in the mesenchyme of mosaic urethra about half of the cells remained unlabelled.

Exposure period: 2 months; X 310

Figs. 42. Urogenital sinuses of wild-type (a) and mosaic (b) sinuses after 4 days' culture in the presence of androgens. Prostatic buds were induced in sinuses of both genotypes. X 430

Figs. 43. Autoradiogrammes of an androgen-untreated fragment of the wild-type female sinus (a) and prostatic buds induced in the fragment treated with androgen for 4 days (b). Almost all mesenchymal cells were labelled. Exposure period: 3 months; X 850 for a and X 440 for b

# PLATE 11



## Explanation of PLATE 12

### Abbreviations

E, sinus epithelium; M, sinus mesenchyme;

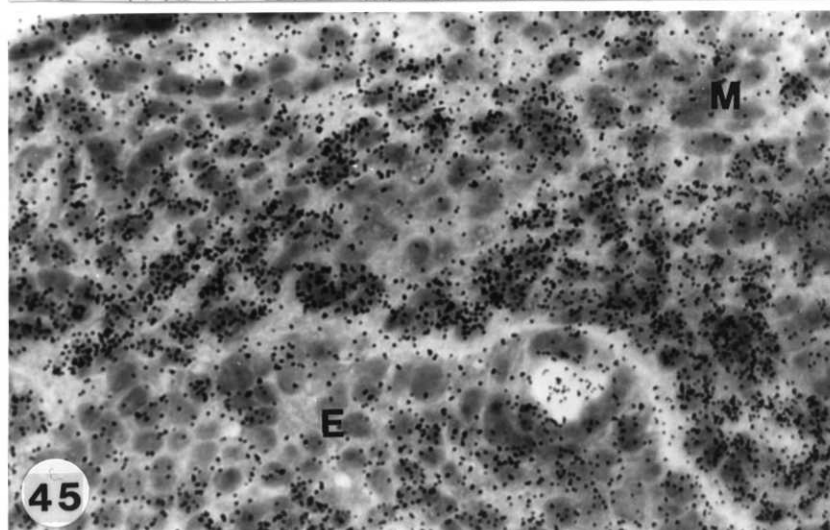
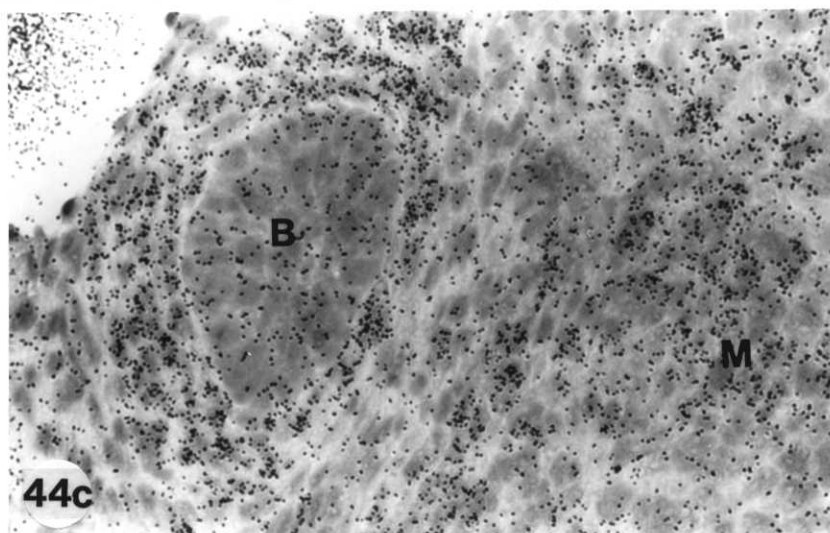
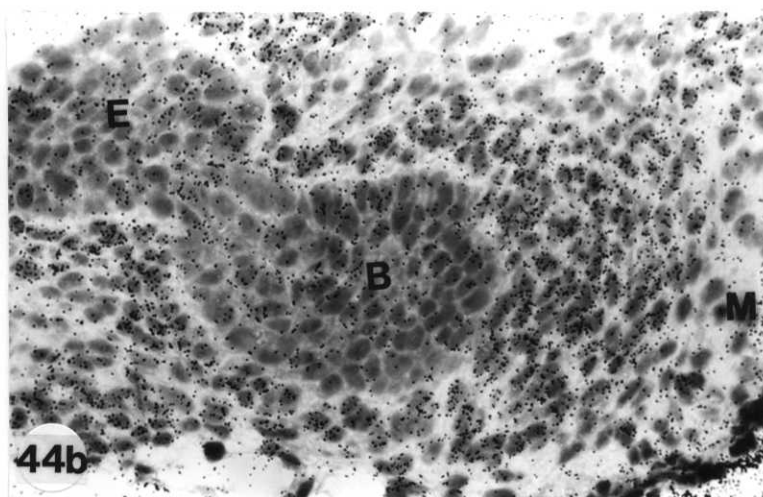
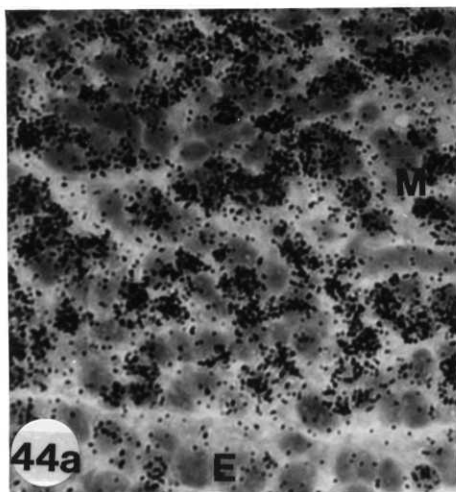
B, prostatic bud

Figs. 44. Autoradiogrammes of an androgen-untreated fragment of the mosaic sinuses (a) and prostatic buds induced in a fragment treated with androgen for 4 days (b, c). In the mesenchyme of the androgen-untreated fragment, labelled and unlabelled cells coexisted near the epithelium, while in the androgen-treated fragment the several layers of mesenchymal cells surrounding the buds consisted of only labelled cells, and mosaicism appeared in outer layers of mesenchyme.

Exposure period: 3 months; X 850 for a, X 440 for b, and X 550 for c

Fig. 45. Autoradiogramme of the mesenchyme surrounding the non-budding area of the sinus epithelium in mosaic sinuses cultured for 4 days in the presence of androgens. The epithelium was surrounded only by labelled cells. Exposure period: 3 months; X 550

# PLATE 12



sinus, disappeared around the developing buds : almost all mesenchymal cells of several layers surrounding the buds exhibited nuclear labelling while in the outer layers labelled and unlabelled cells coexisted (Figs. 44a - c). Moreover, the proportion of labelled cells was greatly increased in the mesenchyme just beneath the non-budding area of the sinus epithelium (Fig. 45).

To investigate whether the increase in the proportion of labelled mesenchymal cells beneath the epithelium has occurred before the onset of bud formation, I exposed the mosaic sinuses to testosterone for 1 day and then cultured them for 1 day in control medium. Under these conditions, about a half of the mosaic sinuses showed 1 or 2 prostatic buds and the others showed no bud yet. Regardless of the appearance of buds, a large part of the epithelium has been already surrounded by the labelled cells in all mosaic sinuses (Figs. 46a and b). Quantitative comparison between androgen-treated and -untreated sinuses confirm this observation (Fig. 49). These results indicated that the proportion of labelled cells beneath the epithelium was greatly increased before prostatic bud induction. Newly induced buds also have been surrounded by a few layers of labelled cells (Fig. 47). In all the experiments, it seemed that the labelled mesenchymal cells surrounding the developing buds were more numerous than those surrounding the non-budding area of the sinus epithelium.

To confirm whether such increase in the proportion of



labelled cells was caused by testosterone added to the medium, the mosaic sinuses were cultured for 2 days in control medium and then processed for steroid autoradiography. These culture conditions could not induce the buds and could not increase the proportion of labelled mesenchymal cells beneath the sinus epithelium (Figs. 48 and 50). This result indicated that testosterone in the medium increased the proportion of labelled cells beneath the epithelium.

### C. Effect of testosterone on the mesenchymal cell proliferation

It is possible that the selective proliferation of the androgen-receptor positive cells account for the increase in the proportion of labelled cells. To test this possibility, I examined the mitotic activity in the mesenchymal cells surrounding the epithelium. The sinuses of all four genotypes ( $X^+/Y$ ,  $X^{Tfm}/Y$ ,  $X^+/X^+$  and  $X^{Tfm}/X^+$ ) were labelled with [ $^3H$ ]thymidine after 1 or 2 days' androgen-treatment, and labelling index was counted in the first layer of mesenchyme. There was no significant difference among 4 genotypes in mitotic activities. Especially the comparisons of the labelling index in the mesenchyme of the wild-type male ( $X^+/Y$ ) and the Tfm mutant ( $X^{Tfm}/Y$ ) have shown that even in the presence of testosterone Tfm mutant (androgen-receptor negative) cells possess the similar activity of proliferation as wild-type (androgen-receptor positive) cells (Figs. 51a

and b, Table 5). The prostatic buds were induced after 2 days' exposure to testosterone and the mesenchymal cells surrounding the developing buds exhibited higher mitotic activity than those surrounding the non-budding area of the sinus epithelium (Fig. 52 and Table 5).

Explanation of PLATE 13

Abbreviations

E, sinus epithelium; M, sinus mesenchyme;

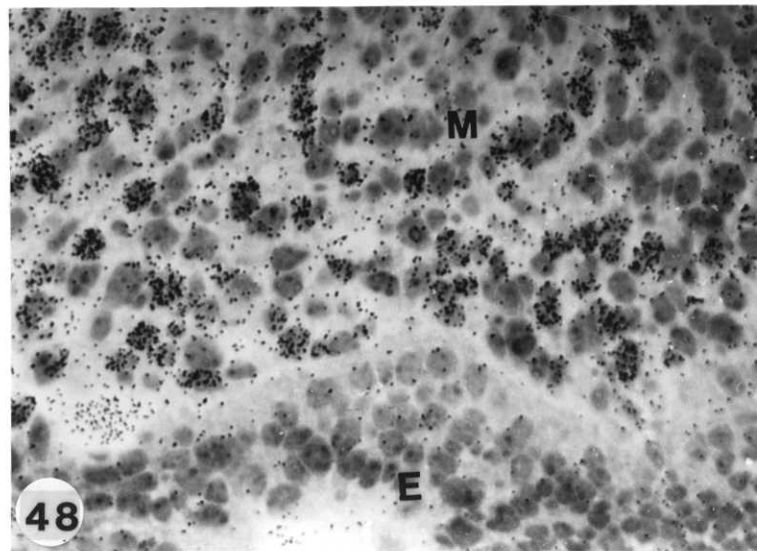
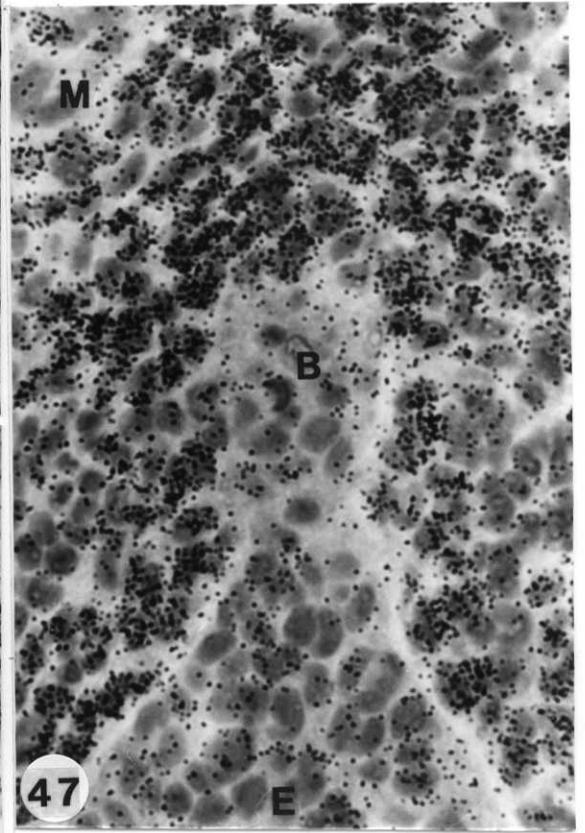
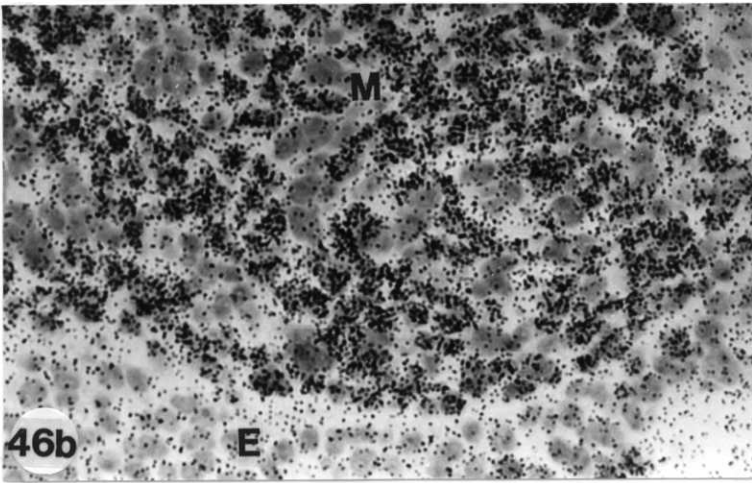
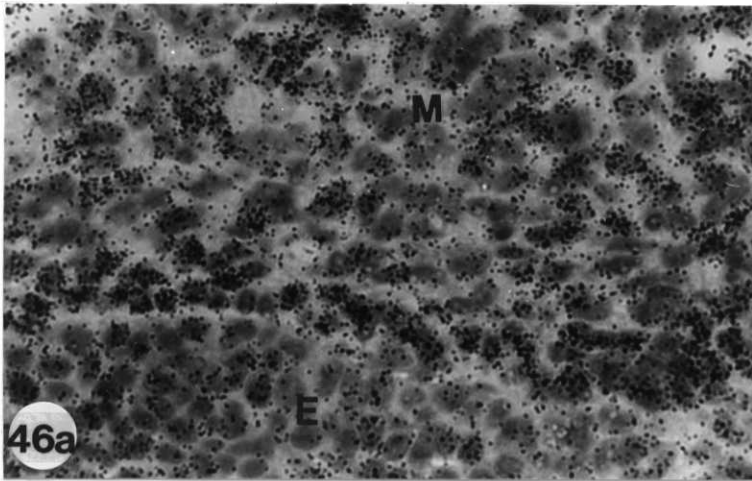
B, prostatic bud

Figs. 46. Autoradiogrammes of mosaic sinus after 2 days' culture in the presence of androgen (a and b). The mesenchyme beneath the epithelium consisted of only labelled cells. Exposure period: 3 months; X 550

Fig. 47. Autoradiogramme of a prostatic bud induced in the mosaic sinus after 2 days' androgen-treatment. The prostatic bud was surrounded by a few layers of labelled cells. Exposure period: 3 months; X 680

Fig. 48. Autoradiogramme of a mosaic sinus cultured for 2 days in the absence of androgens. The mesenchyme beneath the epithelium exhibited mosaicism. Exposure period: 2 months; X 550

# PLATE 13



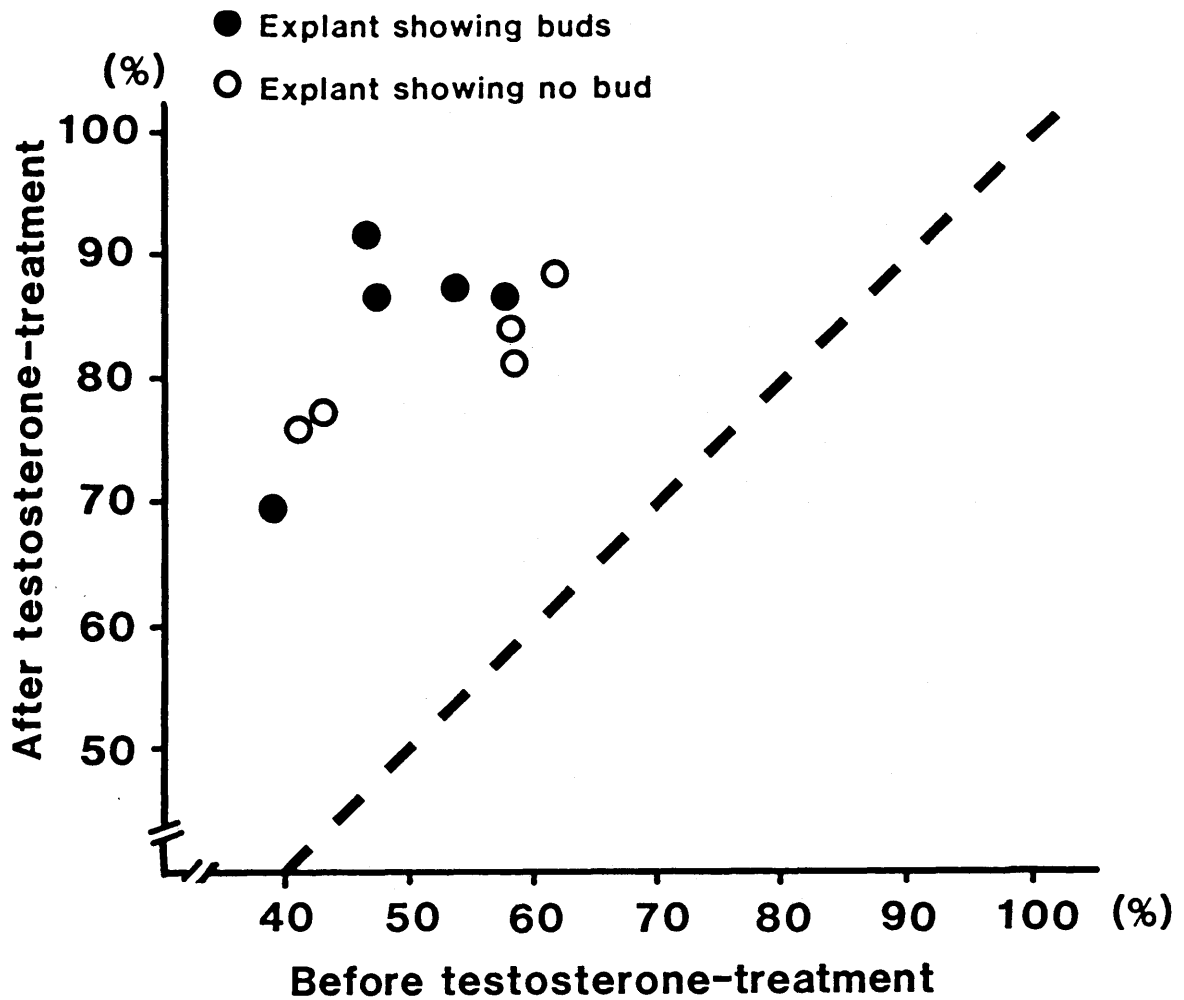


Fig. 49. Proportion of labelled mesenchymal cells to unlabelled ones beneath the epithelium in mosaic sinuses after 2 days' androgen-treatment. Cells in the first layer of the mesenchymal cells beneath the epithelium were counted. The mesenchymal cells possessing more than 7 grains in their nuclei in autoradiogrammes were considered labelled. The proportion of labelled cells to unlabelled cells in the fragment cultured for 2 days in control medium was plotted against that in the corresponding androgen-untreated fragment which has been subjected to autoradiography before cultivation. Solid circle represents the sinus which already has formed a few prostatic buds. Open circle represents the sinus which has not formed bud yet. Broken line represents the line of  $X=Y$ . 3000-4000 mesenchymal cells were counted in each explant.

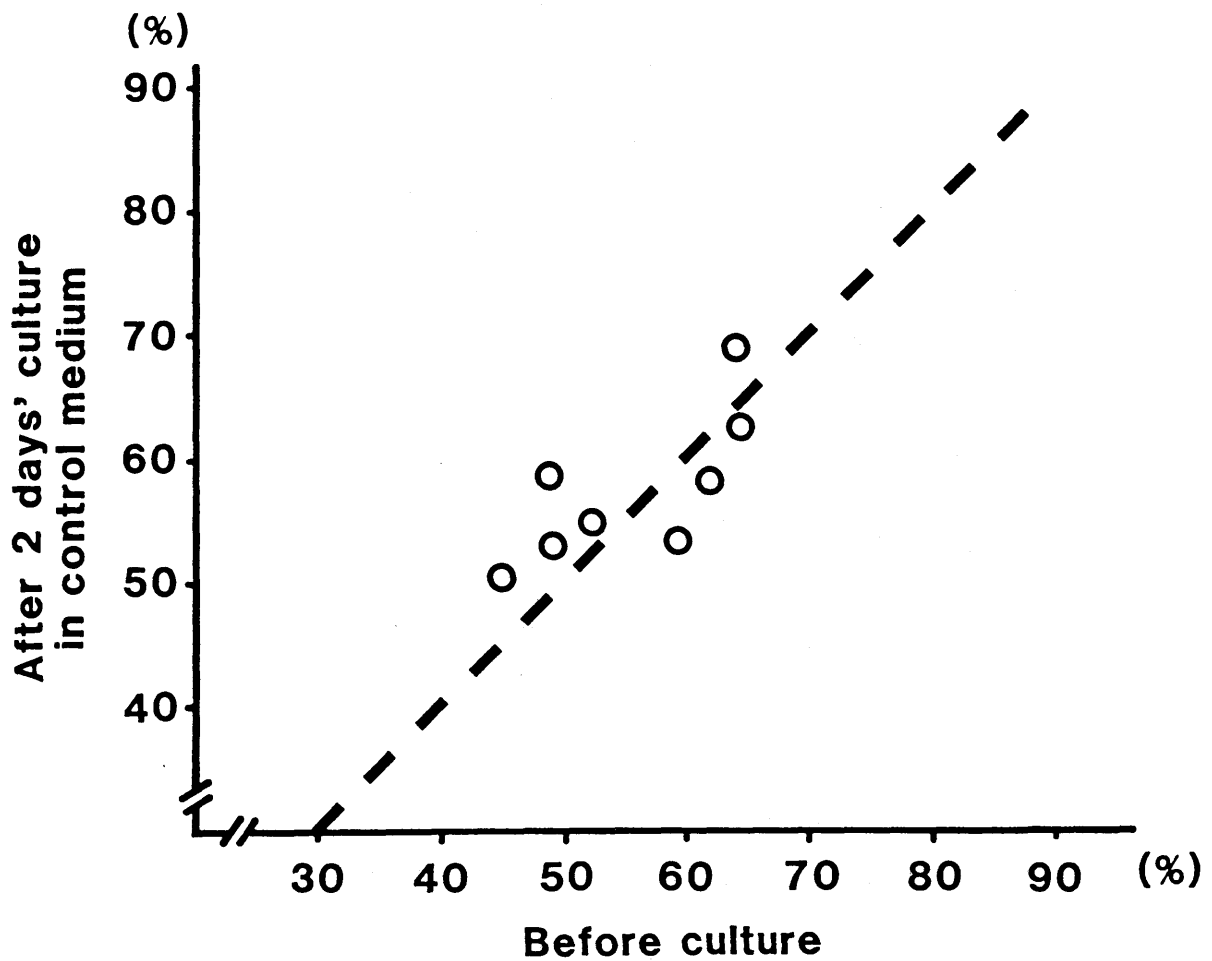


Fig. 50. Proportion of labelled mesenchymal cells to unlabelled ones beneath the epithelium in mosaic sinuses after 2 days' culture in the absence of androgens. Cells in the first layer of the mesenchymal cells beneath the epithelium were counted. The mesenchymal cells possessing more than 7 silver grains in their nuclei in autoradiogrammes were considered labelled. The proportion of labelled cells to unlabelled cells in the fragment cultured for 2 days in control medium was plotted against that in the corresponding androgen-untreated fragment which has been subjected to autoradiography before cultivation. Broken line represents the line of  $X=Y$ . 3000-4000 mesenchymal cells were counted in each explant.

## Explanation of PLATE 14

### Abbreviations

E, sinus epithelium; M, sinus mesenchyme;

MF, Millipore filter

Figs. 51. Autoradiogrammes of [<sup>3</sup>H]thymidine incorporation in the wild-type male (X<sup>+</sup>/Y) (a) and Tfm mutant male (X<sup>Tfm</sup>/Y) (b) sinuses after 2 days' culture in the presence of androgens. The proliferation of the mesenchymal cells beneath the epithelium was <sup>the</sup> same between the sinuses of both genotypes. Expoure period: 5 days; X 440

Fig. 52. Autoradiogramme of [<sup>3</sup>H]thymidine incorporation in an area cross to developing buds. The mesenchymal cells surrounding buds exhibited high proliferative activities (arrows). Exposure period: 5 days; X 440

# PLATE 14

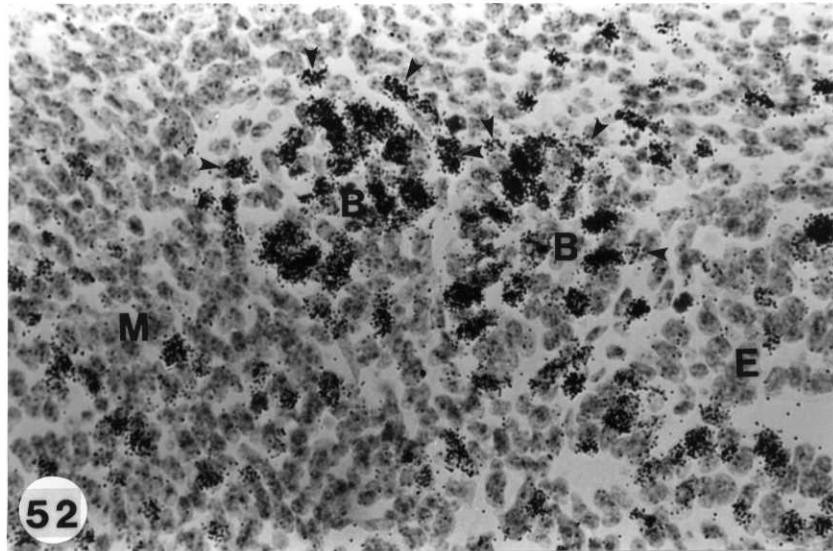
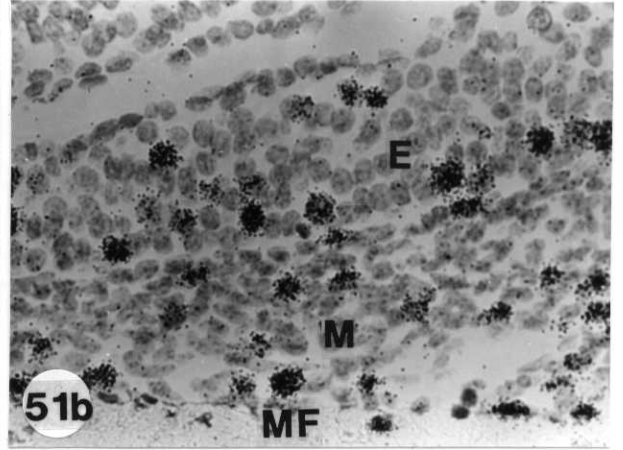
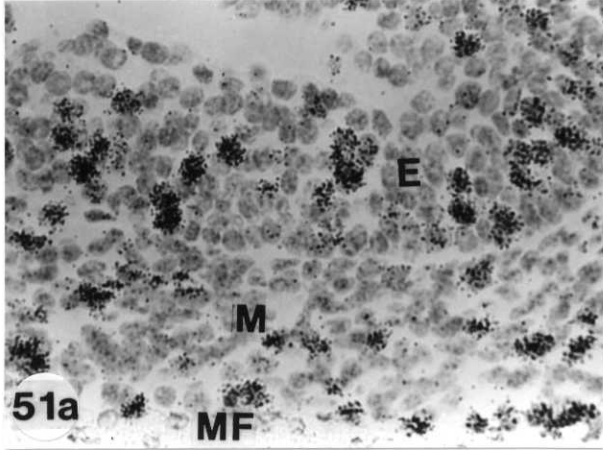




Table 5. Labelling index in the mesenchyme of urogenital sinuses

Phenotype	Genotype	No. of explants	No. of explants showing buds	Labelling Index (Mean $\pm$ S.D.) (%) <sup>*1</sup>
I. 1 day's culture with testosterone				
Wild male <sup>*2</sup>	X <sup>+</sup> /Y	7	0	29.3 $\pm$ 2.5
Tfm mutant male <sup>*2</sup>	X <sup>Tfm</sup> /Y	5	0	32.2 $\pm$ 1.6
Wild female <sup>*3</sup>	X <sup>+</sup> /X <sup>+</sup>	4	0	30.4 $\pm$ 1.8
Mosaic female <sup>*3</sup>	X <sup>Tfm</sup> /X <sup>+</sup>	8	0	29.8 $\pm$ 2.3
II-A. 2 days' culture with testosterone: Mesenchyme surrounding the non-budding area of the sinus epithelium				
Wild male	X <sup>+</sup> /Y	11	9	12.5 $\pm$ 1.2
Tfm mutant male	X <sup>Tfm</sup> /Y	8	0	12.6 $\pm$ 1.3
Wild female	X <sup>+</sup> /X <sup>+</sup>	2	2	10.4
Mosaic female	X <sup>Tfm</sup> /X <sup>+</sup>	6	6	13.5 $\pm$ 1.1
II-B. 2 days' culture with testosterone: Mesenchyme surrounding the elongating buds				
Wild male	X <sup>+</sup> /Y	9 <sup>*4</sup>	-	33.6 $\pm$ 6.8

Legend for Table 5.

- \*1 The first layer of the mesenchymal cells surrounding the epithelium was counted. 3000-5000 cells were counted in each explant except II-B.
- \*2 Male genotype was determined by the histological observation of mammary gland rudiments.
- \*3 Female genotype was determined by steroid autoradiography of the fragment of each sinus before incubation with testosterone. The sinuses where more than 90% of mesenchymal cells were labelled were considered wild-type.
- \*4 27 buds from 9 explants were examined.

## Discussion

In the present study X-inactivation mosaicism concerning Tfm gene could be visualized by means of steroid autoradiographic techniques. Since the tissues of female mice have not been exposed to endogenous androgen before explantation (Habert and Picon, 1984), it is reasonable to assume that cell selection does not favour only one of the two cell types. This assumption is supported by the fact that the proportion of receptor-positive and -negative cells does not significantly deviate from 50% (Table 3).

One-dimensional analysis of West revealed that in the mosaic mesenchyme the estimated coherent clone size was very small (2-3 nuclei per coherent clone). Since this one-dimensional analysis assumes non-differential proliferation, random distribution of progenitor cells and a regular shape of coherent clones, the derived mean clone size will be a minimum estimate. However, the small coherent clone size in the urogenital mesenchyme suggests either small coherent clones or larger highly branched ones. Both of these alternatives imply that considerable cell mixing occurred during fetal development. These results are not confined to the urogenital mesenchyme but are comparable to those reported by West (1976a) for retinal epithelium of fetal mouse (2.24 cells per clone at 15.5 days of gestation), suggesting that cell mixing occurs during mammalian fetal development in general.

In the present investigation, these mosaic sinuses were used for the study of the behaviour of mesenchymal cells during prostatic morphogenesis. The in vitro culture of mosaic female sinuses with androgen resulted in a substantial increase in the proportion of labelled mesenchymal cells beneath the epithelium. This increase in the number of labelled cells has been already observed before the appearance of prostatic buds within the epithelium. However, the culture without androgen could not produce such an increase. It is apparent, therefore, that androgens added to the medium increase the proportion of labelled mesenchymal cells beneath the epithelium and thereafter epithelial buds develop. For the explanations of this characteristic increase in the number of labelled cells, at least three possibilities could be considered: First, androgens stimulate the cell proliferation of androgen-receptor positive cells. Second, androgens promote the selective death of receptor-negative cells. Finally, androgens influence the behaviour of androgen-receptor positive cells, such as direction of movement of the cells or affinity to the epithelium. The first possibility can be excluded by the results obtained in the present investigation that the difference of mitotic activities between wild-type and Tfm mutant cells could not be detected even in the presence of androgens. The second possibility seems unlikely because the cell death was hardly observed in the sinuses of all genotypes during the cultivation in

vitro with androgens, and also in the sinuses in the course of normal embryonic development. Therefore, the last possibility is most plausible: That is, before the onset of bud formation the androgen-primed mesenchymal cells behave so as to surround the epithelium. It is possible that the mesenchymal cells which incorporate androgens would be apt to move to the epithelium or to stay near the epithelium for a long period. As already demonstrated, the mesenchymal cells were considerably mixed with each other, and this result suggests that a subtle difference of the behaviour between two types of cells might result in observed cell selection beneath the epithelium. This behaviour of mesenchymal cells may assure the contacts between epithelial and mesenchymal cells and play a decisive role in epithelial-mesenchymal interaction. In fact, that the inductive interactions require close cell contact has been established by transfilter experiments in many systems: the induction of kidney tubules (Wartiovaara, Nordling, Lehtonen and Saxén, 1974; Lehtonen, Wartiovaara, Nordling, and Saxén, 1975), the induction of odontoblast in mammalian tooth morphogenesis (Thesleff, Lehtonen, Wartiovaara and Saxén, 1977), and the induction of cartilage in avian limb mesoderm (Gumpel-Pinot, 1980 and 1981).

In the present study, I found that the developing buds in the mosaic sinuses were always surrounded by several layers of labelled cells. This may indicate that mesenchymal cells not only stimulate the epithelium to form

buds but also actively participate in the bud elongation. Thymidine labelling experiments revealed that the mesenchymal cells around the epithelium exhibited higher level of mitotic activity than those surrounding the non-budding area of the siuns epithelium. These results suggest that the characteristic localization of labelled cells around buds arises by the selective proliferation of receptor-positive cells. However, I could not further examine this possibility because there is no technique to confirm whether the cell in proliferation is receptor-positive. Therefore, the other possibilities such as the migration of receptor-positive cells from more distant sites or the involvement of receptor-positive cells which happen to encounter elongating buds can not be excluded.

Prostatic bud induction and bud elongation proceed normally in mosaic sinuses. However, only several layers of receptor-positive mesenchymal cells surrounding the epithelium seemed to participate in those processes. These observations emphasize the importance of the mesenchyme just beneath the epithelium in prostatic morphogenesis. In mammary gland the similar result has been obtained by Dürnberger et al (1978). Androgen-dependent regression requires only 2 to 3 layers of androgen-sensitive mesenchymal cells surrounding mammary buds. These results suggest that androgens exert their effects on the epithelium through the mesenchymal cells present in close vicinity to the epithelium.

Finally, by combination of  $X^{Tfm}/X^+$  heterozygous mosaic sinuses and steroid autoradiographic technique, I could demonstrate the behaviour of the mesenchymal cells at the epithelio-mesenchymal interface. The present study is expected to provide the important information on the mechanism of tissue interaction in organogenesis.

## Summary

By combination of steroid autoradiographic technique and the use of Tfm mosaic female sinuses ( $X^{Tfm}/X^+$ ), X-chromosome mosaicism could be visualized. Changes in mosaic pattern after androgen-treatment was pursued and the behaviour of androgen-receptor positive mesenchymal cells during prostatic bud induction was examined.

1. In the sinus mesenchyme of wild-type female fetuses ( $X^+/X^+$ ), more than 95% of the cells were androgen-receptor positive. In the sinus mesenchyme of heterozygous female fetuses ( $X^{Tfm}/X^+$ ), about a half of the cells were receptor-positive (Tfm gene inactive), and both receptor-positive and receptor-negative cells coexisted in small irregular patches, suggesting that considerable cell mixing occurs in the sinus mesenchyme during embryonic development.
2. When the mosaic sinuses were cultured in vitro in the presence of androgen, the prostatic buds were induced. The number of induced buds reached to as much as 70% of those in wild-type female sinuses.
3. Autoradiographic analysis revealed that the induced buds in mosaic sinuses were surrounded by several layers of receptor-positive mesenchymal cells; the mosaicism disappeared around the buds. Moreover, the proportion of androgen-receptor positive cells was greatly increased in the mesenchyme just beneath the non-budding area of the



sinus epithelium. This increase was induced by androgen added to the medium and has been already observed before the onset of bud formation.

4. It was demonstrated that selective proliferation of androgen-receptor positive cells and selective death of receptor negative cells were not involved in the increase in proportion of receptor-positive cells beneath the epithelium. These findings indicate that the mesenchymal cells near the epithelium behave so as to surround the epithelium after they incorporate androgens in their nuclei.
5. The mesenchymal cells around elongating buds in mosaic sinuses exhibited higher mitotic activity, suggesting the possibility that the selective proliferation of receptor-positive cells occurs in the mesenchyme surrounding buds.

The results are discussed in relation to a possible role of the behaviour of mesenchymal cells in epithelial-mesenchymal interaction.

## GENERAL CONCLUSION

\*\*\*\*\*

In the present thesis, I investigated the androgen-induced epithelial-mesenchymal interaction in prostatic morphogenesis by means of steroid autoradiographic techniques.

A. One of the most important conclusions of the thesis is that the prostatic morphogenesis is induced by the androgen-activated mesenchyme. This was elucidated from the following results.

1. The uptake of androgens by the fetal rat urogenital sinus was restricted to the mesenchyme surrounding the epithelium which showed no uptake of androgens. At 18.5 days of gestation, prostatic buds developed from the sinus epithelium but they remained negative for androgen-incorporation.

2. The relationship between androgen-incorporation into the mesenchyme and prostatic bud formation was demonstrated in the experiments of brief androgen-treatment. Prostatic bud formation occurs only when the mesenchymal cells incorporate a certain amount of androgens in their nuclei and it ceases just after the disappearance of the androgens

in the mesenchymal cells.

3. Uptake of androgens by the prostatic bud epithelium was first seen at 10 days after birth, preceding its functional differentiation. This suggested that the epithelial androgen receptors would play a decisive role in the functional differentiation of the prostatic epithelium. However, recombination experiments of Tfm epithelium and wild-type mesenchyme revealed that even in the absence of epithelial androgen receptors the mesenchyme which incorporated androgens could induce the epithelium to form a prostate-like glandular morphology and also to express some characteristic enzymes.

B. The other important conclusion of the present thesis is that during the epithelial bud induction, the mesenchymal cells near the epithelium behave so as to surround the epithelium after they incorporate androgens in their nuclei. This conclusion was obtained in the experiments with X-inactivation mosaicism concerning Tfm gene expression. In the sinus mesenchyme of  $X^{Tfm}/X^+$  heterozygous female mice, the androgen-receptor positive and negative cells coexisted in small irregular patches. Moreover, the prostatic buds were induced in such mosaic sinuses when they were cultured in vitro in the presence of androgens. By the chase of changes in mosaic pattern after androgen-treatment, it was revealed that androgens increased the proportion of receptor-positive mesenchymal cells beneath the epithelium, and thereafter

epithelial buds developed. It was also demonstrated that the selective proliferation of receptor-positive cells and selective death of receptor-negative cell did not occur near the epithelium before the onset of prostatic bud formation. From these results it was concluded that the androgens alter the behaviour of mesenchymal cells at epithelio-mesenchymal interface so that they surround the epithelium during the prostatic bud induction. This behaviour of mesenchymal cells may play an important role in the epithelial-mesenchymal interaction by assuring the close contact between the epithelial and mesenchymal cells.

I also found in the present investigation that the elongating buds in the mosaic sinuses were always surrounded by several layers of receptor-positive mesenchymal cells. This result suggests that the androgen-activated mesenchymal cells does not only stimulate the epithelium to form buds but also actively participate in the epithelial bud elongation.

Thus, by steroid autoradiographic techniques, the present thesis revealed the androgen-target tissue and the cell behaviour in the mesenchyme during prostatic morphogenesis. These studies seem to provide a new insight into the problems of hormone-dependent tissue-interaction.

## REFERENCES

\*\*\*\*\*

- Abercrombie, M. (1946). Estimation of nuclear population from microtome sections. Anatomical Record, 94, 239-247.
- Blondeau, J. P., Corpechot, C., Le Goascogne, C., Baulieu, E. E. and Robel, P. (1975). Androgen receptor in the rat ventral prostate and their hormonal control. Vitamines and Hormones, 33, 319-350.
- Blondeau, J.-P., Baulieu, E.-E. and Robel, P. (1982). Androgen-dependent regulation of androgen nuclear receptor in the rat ventral prostate. Endocrinology, 110, 1926-1932.
- Boesel, R. W., Klipper, R. and Shain, S. A. (1980). Androgen regulation of androgen receptor content and distribution in the ventral and dorsolateral prostates of aging AXC rats. Steroids, 35, 157-177.
- Bullock, L. P. and Bardin, C. W. (1974). Androgen receptors in mouse kidney: a study of male, female and androgen-insensitive (Tfm/Y) mice. Endocrinology, 94, 746-756.
- Condamine, H., R. P. Custer, and B. Mintz (1971). Pure-strain and genetically mosaic liver tumors histochemically identified with the  $\beta$ -glucuronidase marker in allophenic mice. Proceedings of National Academy of Science of

the U. S. A., 79, 2957-2961.

Cunha, G. R. and Lung, B. (1978). The possible influence of temporal factors in androgenic responsiveness of urogenital tissue recombinants from wild-type and androgen-insensitive (Tfm) mice. Journal of Experimental Zoology, 205, 181-194.

Cunha, G. R., Shannon, J. M., Neubauer, B. L., Sawyer, L. M., Fujii, H., Taguchi, O. and Chung, L. W. K. (1981). Mesenchyme-epithelial interactions in sex differentiation. Human Genetics, 58, 58-77.

Cunha, G. R., Shannon, J. M., Vanderslice, K. D., Shekkingstad, M. and Robboy, S. J. (1982). Autoradiographic analysis of nuclear estrogen binding sites during postnatal development of the genital tract of female mice. Journal of Steroid Biochemistry, 17, 281-286.

Delettré, J., Mornon, J. P., Lepicard, G., Ojasoo, T. and Raynaud, J. P. (1980). Steroid flexibility and receptor specificity. Journal of Steroid Biochemistry, 13, 45-49.

Dürnberger, H., Heuberger, B., Schwartz, P., Wasner, G. and Kratochwil, K. (1978). Mesenchyme-mediated effect of testosterone on embryonic mammary epithelium. Cancer Research, 38, 4066-4070.

Gumpel-Pinot, M. (1980). Ectoderm and mesoderm interactions in the limb bud of the chick embryo studied by transfilter cultures: cartilage differentiation and ultrastructural observations. Journal of Embryology and Experimental

- Morphology, 59, 157-173.
- Gumpel-Pinot, M. (1981). Ectoderm-mesoderm interactions in relation to limb-bud condensation in the chick embryo: transfilter cultures and ultrastructural studies. Journal of Embryology and Experimental Morphology, 65, 73-87.
- Häbert, R. and Picon, R. (1984). Testosterone, dihydrotestosterone and estradiol-17 $\beta$  levels in maternal and fetal plasma and in fetal testes in the rat. Journal of Steroid Biochemistry, 21, 193-198.
- Heuberger, B., Fitzka, I., Wasner, G. and Kratochwil, K. (1982). Induction of androgen receptor formation by epithelium-mesenchyme interaction in embryonic mouse mammary gland. Proceedings of National Academy of Science of the U. S. A., 79, 2957-2961.
- Jost, A. (1965). Gonadal hormones in the sex differentiation of the mammalian fetus. In Organogenesis, pp.611-628. Eds. Haan, R. L. and Ursprung, H. Holt, Rinehart and Wilson, New York.
- Kratochwil, K (1977). Development and loss of androgen responsiveness in the embryonic rudiment of mouse mammary gland. Developmental Biology, 61, 358-365.
- Lasnitzki, I. (1965). Action and interaction of hormones 3-methylcholanthrene on the ventral prostate gland of the rat in vitro. Journal of the National Cancer Institute, 35, 339-348.
- Lasnitzki, I. and Mizuno, T. (1977). Induction of the rat prostate gland by androgens in organ culture. Journal of

- Endocrinology, 74, 47-55.
- Lasnitzki, I. and Mizuno, T. (1979). Role of the mesenchyme in the induction of the rat prostate gland by androgen in organ culture. Journal of Endocrinology, 82, 171-178.
- Lasnitzki, I. and Mizuno, T. (1980a). Prostatic induction: interaction of epithelium and mesenchyme from normal wild-type mice and androgen-insensitive mice with testicular feminization. Journal of Endocrinology, 85. 423-428.
- Lasnitzki, I. and Mizuno, T. (1980b). Antagonistic effects of cyproterone acetate and oestradiol on the development of the fetal rat prostate gland induced by androgen in organ culture. The Prostate, 1, 147-156.
- Lehtonen, E., Wartiovaara, J., Nordling, S., and Saxén, L. (1975). Demonstration of cytoplasmic processes in Millipore filters permitting kidney tubule induction. Journal of Embryology and Experimental Morphology, 33, 187-203.
- Lodja Z., Grossrau R. and Shiebler T. H. (1979). Enzyme Histochemistry, Springer-Verlag, Berlin.
- Lyon, M. F. (1961). Gene action in the X-chromosome of the mouse (Mus musculus L.). Nature, 190, 372-373.
- Mainwaring, W. I. P. (1969). A soluble androgen receptor in the cytoplasm of rat prostate. Journal of Endocrinology, 45, 531-541.
- Monk, M., and M. I. Harper (1979). Sequential X chromosome inactivation coupled with cellular differentiation in



- early mouse embryos. Nature, 281, 311-313.
- Mystkowska, E. T., and A. K. Tarkowski (1968). Observations on CBA-p/CBA-T6T6 mouse chimeras. Journal of Embryology and Experimental Morphology, 20, 33-52.
- Naftolin, F., Ryan, K. J., Davies, I. J., Reddy, V. V., Flores, F., Petro, Z. and Kuhn, M. (1975). The formation of estrogen by central neuroendocrine tissues. Recent Progress in Hormone Research, 31, 295-319.
- Perel, E. and Killinger, W. (1983). The metabolism of androstenedione and testosterone to C<sub>19</sub> metabolites in normal breast, breast carcinoma and benign prostatic hypertrophy tissue. Journal of Steroid Biochemistry, 19, 1135-1139.
- Picon, R. (1976). Testosterone secretion by foetal rat testes in vitro. Journal of Endocrinology, 71, 231-238.
- Shindler, A. E. (1975). Steroid metabolism of fetal tissues;II. conversion of androstenedione to estrone. American Journal of Obstetrics and Gynecology, 123, 265-268.
- Saxén, L., Karkinen-Jaaskeläinen, M., Lehtonen, E., Nordling, S. and Wartiovaara, J. (1976). Inductive tissue interactions. In Cell surface reviews volume 1, pp. 331-407, Eds G. Poste and G. L. Nicolson. North-Holland Publishing Company, Amsterdam.
- Shannon, J. M., Cunha, G. R., Taguchi, O., Vanderslice, K. D. and Gould S. F. (1982). Autoradiographic localization of steroid binding in human tissue labeled in vitro.

- Journal of Histochemistry and Cytochemistry, 30, 1059-1065.
- Shannon, J. M. and Cunha, G. R. (1983). Autoradiographic localization of androgen binding in the developing mouse prostate. The Prostate, 4, 367-373.
- Sheridan, P. J., Buchanan, J. M. and Anselmo, V. (1981). Autoradiographic and biochemical studies of hormone receptor localization. Journal of Histochemistry and Cytochemistry, 29, 195-200.
- Shiojiri, N. and Mizuno, T. (1981). Mesenchymal Alkaline phosphatase in rat prostatic bud formation. Development, Growth and Differentiation, 23, 460.
- Stumpf, W. E. (1968). High-resolution autoradiography and its application to in vitro experiments: subcellular localization of <sup>3</sup>H-estradiol in rat uterus. In Radioisotopes in Medicine: In Vitro Studies, pp. 633-660. Eds. Hayes, R. J., Goswitz, F. A and Murphy, B. E. P. U. S. Atomic Energy Commission, Oak Ridge, Tenn.
- Stumpf, W. E. and Sar, M. (1975). Autoradiographic techniques for localizing steroid hormones. Methods in Enzymology, 36, 135-156.
- Stumpf, W. E., Narbaitz, R. and Sar, M. (1980). Estrogen receptors in the fetal mouse. Journal of Steroid Biochemistry, 12, 55-64.
- Takasugi, N. (1976). Cytological basis for permanent vaginal changes in mice treated neonatally with steroid hoemones. International review of cytology, 44, 193-224

- Thesleff, I., Lehtonen, E., Wartiovaara, J. and Saxén, L. (1977). Interference of tooth differentiation with interposed filters. Developmental Biology, 58, 197-203.
- Trowell, O. A. (1959). The culture of mature organs in a synthetic medium. Experimental Cell Research, 16, 118-148.
- Warren, D. W., Haltmeyer, G. C. and Eik-Nes, K. B. (1973). Testosterone in the fetal rat testis. Biology of Reproduction, 8, 560-565.
- Wartiovaara, J., Nordling, S., Lehtonen, E. and Saxén, L. (1974). Transfilter induction of kidney tubules: correlation with cytoplasmic penetration into Nucleopore filters. Journal of Embryology and Experimental Morphology, 31, 667-682.
- Wasner, G., Hennermann, I. and Kratochwil, K. (1983). Ontogeny of mesenchymal androgen receptor in the embryonic mouse mammary gland. Endocrinology, 113, 1171-1180.
- Wessells, N. K. (1977). Tissue Interactions in Development, W. A. Benjamin, Menlo Park.
- West, J. D. (1975). A theoretical approach to the relation between patch size and clone size in chimaeric tissue. Journal of theoretical Biology, 50, 153-160.
- West, J. D. (1976a). Clonal development of the retinal epithelium in mouse chimaeras and X-inactivation mosaics. Journal of Embryology Experimental Morphology, 35, 445-461.
- West, J. D. (1976b). Patches in livers of chimaeric mice.

Journal of Embryology Experimental Morphology, 36, 151-161.

Wilson, J. D., Griffin, J. M., George, F. W. and Leshin, M. (1981). The role of gonadal steroids in sexual differentiation. Recent Progress in Hormone Research, 37, 1-39.

Zahar, T. and Toth, M. (1982). Steroid binding properties of the rat seminal vesicle androgen receptor: short-term and long-term competition of various steroids with radioactive dihydrotestosterone. Journal of Steroid Biochemistry, 17, 287-293.

PUBLISHED PAPERS

\*\*\*\*\*

Takeda, H. and Mizuno, T. (1984). Incorporation des androgenes au moment de la cytodifférenciation de l'épithélium prostatique chez le Rat. Comptes Rendus de Séances de la Société de Biologie, 178, 572-575.

Takeda, H., Mizuno, T. and Lasnitzki, I. (1985). Autoradiographic studies of androgen-binding sites in the rat urogenital sinus and postnatal prostate. Journal of Endocrinology, 104, 87-92.

Takeda, H., Lasnitzki, I. and Mizuno, T. (1986). Analysis of prostatic bud induction by brief androgen treatment in the fetal rat urogenital sinus. Journal of Endocrinology, 110, 567-470.

Takeda, H., Suzuki, M., Lasnitzki, I. and Mizuno, T. (1987). Visualization of X-chromosome inactivation mosaicism of Tfm gene in  $X^{Tfm}/X^+$  heterozygous female mice. Journal of Endocrinology, in press.

Takeda, H., Lasnitzki, I. and Mizuno, T. (1987). Change of mosaic pattern by androgens during prostatic bud formation in  $X^{Tfm}/X^+$  heterozygous female mice. Journal of Endocrinology, in press.